of the serum GH, IGF-1, and IGFBP-3 assay was 0.02 ng/ml, 4 μg/l, and 0.20 mg/l, respectively. The GH/IGF-1, GH/IGFBP-3, and IGF-1/IGFBP-3 concentration ratios were estimated to get a better understanding of the relative changes in concentration of GH, IGF-1, and IGFBP-3.

Statistical analysis

Data were processed on a personal computer and analyzed using StatView 5.0 (SAS Institute, Inc., Cary, NC). Differences between groups were analyzed by Mann–Whitney test and Pearson χ^2 test. Correlation analysis was carried out using Spearmen rank correlation. Logistic regression analysis was used to test the association of variables with different stages of NAFLD and steatosis. All data in the text and tables are given as means, unless otherwise indicated. Variables that achieved statistical significance in the univariate analysis were subsequently included in a multivariate analysis using a logistic regression model, and described as odds ratios (OR) with 95% CI. Spearman rank correlation was used to examine the relationship between variables. Values of $P < 0.05$ were considered statistically significant.

Results

Subject characteristics

Clinical and laboratory data for the 52 NAFLD subjects are shown in Table 1. BMI (kg/m^2) was distributed as follows: BMI<25 in eight cases; BMI 25–30 in 27 cases; BMI 30–35 in 13 cases, BMI 35–40 in three cases, and BMI >40 in one case. The HOMA-IR score reflects insulin resistance, with a score of >2.5 indicating insulin resistance in Japanese subjects [17]. The mean HOMA-IR index in our subjects was 4.05, and 26 cases (70%) had values in excess of 2.5. The normal range of serum GH concentration is <0.17 ng/ml in males and 0.28–1.64 ng/ml in females. Of the 35 females with NAFLD in the study, 24 (73%) had GH levels less than the normal range, while in the others this was within the normal limits. In contrast, 11 of the 20 male NAFLD patients (58%) had GH levels above the normal range for males, and the remaining eight cases (42%) were within the normal limits. For IGF-1, the normal ranges in males aged 17–20, 21–30, 31–40, 41–50, 51–60, 61–70 and >70-years-old are 219–509, 85–369, 67–318, 41–272, 59–215, 42–250, 75–218 μg/l, respectively, whereas in females these data are 264–542, 119–389, 73–311, 46–282, 37–266, 37–150, 38–207 μg/l, respectively. In this study, three patients (one male and two female) had IGF-1 levels below the normal range for their age, and two patients (both females) had IGF-1 levels higher than the normal range. Regarding IGFBP-3, the normal ranges in people aged 17–35 and 36–70 years old were 2.29–4.17 and 2.17–4.05 mg/l, respectively, and 12 female patients (35%) and seven male patients (37%) had IGFBP-3 levels less than the normal limit for their age. Hence, aberrant values of serum IGF-1 concentration were found in a few cases, IGFBP-3 levels lower than the normal range were found in more than 30% of NAFLD patients.

Clinical and laboratory data in NAFLD patients at stages 0–1 and 2–3

The NAFLD patients who were classified into stages and clinical and laboratory data were compared between stage 0–1 and stage 2–3 patients (Table 1). There were no differences in sex, age, BMI, ALT, γ-GTP, ALP, total cholesterol, triglyceride, C-reactive protein, white blood cell count, red blood cell count, GH, IGFBP-3, insulin, HOMA-IR score, and HbA1c between the two groups. However, AST ($P = 0.0005$) and AST/ALT ($P = 0.0206$) were lower in stage 0–1 patients, and platelet count ($P = 0.002$) and IGF-1 ($P = 0.0272$) were higher in stage 0–1 patients, compared to stage 2–3 patients.

Univariate and multivariate analysis of risk factors for stage 2–3 NAFLD

The results of univariate and multivariate analyses of risk factors for stage 2–3 NAFLD are shown in Table 2. In the univariate analysis, the following three factors were significantly associated with stage 2–3 NAFLD: reduced AST (relative risk (RR), 0.238; 95% confidence interval (CI), 0.069–0.824 [$P = 0.0235$]), reduced platelet count (RR, 4.667; 95% CI, 1.301–16.739 [$P = 0.0181$]), and reduced IGF-1 level (RR, 4.643; 95% CI, 1.331–16.196 [$P = 0.016$]). In a multivariable analysis, reduced platelet count (RR, 5.899; 95% CI, 1.288–27.017 [$P = 0.0223$]) and reduced IGF-1 (RR, 4.568; 95% CI, 1.101–18.945 [$P = 0.0363$]) were significantly associated with stage 2–3 NAFLD.

Correlation between serum hyaluronic acid and the GH/IGF-1/IGFBP-3 axis

Hyaluronic acid is a hepatic fibrosis marker [18], and its correlation with GH, IGF-1 and IGFBP-3 was explored in 41 NAFLD patients in whom the level was within the detection range of the assay (Table 3). The GH level showed no correlation with hyaluronic acid, but IGF-1 and IGFBP-3 levels showed a negative correlation with the hyaluronic acid level, with the IGF-1 level showing a

Table 1 Clinical and laboratory data for NAFLD patients at stages 0–1 and 2–3

Item	Total (n = 52)	Stage 0–1 (n = 34)	Stage 2–3 (n = 18)	P-value
Sex (M/F)	19/33	13/21	6/12	NS
Age (year)	49.7 (17.1)	47.5 (16.7)	55.4 (17.5)	NS
BMI (kg/m^2)	29.0 (4.12)	29.2 (4.4)	28.7 (3.6)	NS
ALT (IU/l)	93.5 (79.1)	76.3 (53.0)	126.0 (107.8)	NS
AST (IU/l)	62.0 (49.8)	45.3 (25.2)	93.7 (67.8)	0.0005
AST/ALT	0.714 (0.226)	0.67 (0.20)	0.80 (0.26)	0.0206
γ-GTP (IU/l)	85.7 (87.2)	67.4 (46.2)	120.3 (129)	NS
ALP (IU/l)	239.0 (71.7)	234.8 (69.3)	246.8 (77.6)	NS
Total cholesterol (mg/dl)	203.1 (35.5)	209.4 (37.6)	191.5 (28.7)	NS
Triglyceride (mg/dl)	161.2 (65.8)	161.1 (64.1)	161.5 (70.7)	NS
C-reactive protein (mg/dl)	0.26 (0.25)	0.251 (0.292)	0.271 (0.187)	NS
White blood cells (μl)	6482 (1664)	6641 (1628)	6683 (1737)	NS
Red blood cells (10^4/μl)	465 (54.6)	473 (45.7)	452 (67.6)	NS
Ferritin (mg/dl)	322 (412.2)	247 (162)	415 (619)	NS
Platelets (μl)	23300 (6300)	24800 (6378)	20400 (5119)	0.002
GH (ng/ml)	0.31 (0.36)	0.298 (0.374)	0.331 (0.357)	NS
IGF-1 (μg/l)	171 (111.8)	191.8 (128)	129.2 (45.4)	0.0272
IGFBP-3 (mg/l)	2.45 (0.66)	2.56 (0,73)	2.24 (0.42)	NS
Insulin (IU/l)	14.8 (6.88)	13.9 (5.56)	16.4 (9.03)	NS
Fasting plasma glucose (mg/l)	113.0 (33.3)	109.4 (30.4)	119.8 (38.4)	NS
HOMA-IR	4.03 (2.4)	3.86 (2.18)	4.40 (2.88)	NS
HbA1c (%)	6.70 (1.9)	6.77 (2.09)	6.48 (1.63)	NS

Data are shown as means (standard deviation) and numbers, with statistical analysis using a Mann–Whitney test for means and a Pearson χ^2 test for numbers

Normal values in laboratory tests: ALT (IU/l), 5–40; AST (IU/l), 10–40; γ-GTP (IU/l), <70 in males, <30 in females; ALP (IU/l), 115–359; total cholesterol (mg/dl), 150–219; triglyceride (mg/dl), 50–149; C-reactive protein (mg/dl), <0.30; white blood cell count (μl), 3900–9800 in males, 3500–9100 in females; red blood cell count (10^4/μl), 427–570 in males, 376–500 in females; ferritin (mg/dl), 27–320 in males, 3.4–89 in females; platelet (μl), 13.1–36.2 in males, 13–36.9 in females; insulin (IU/l), 3.06–16.9; fasting plasma glucose (mg/l), 70–109; HbA1c (%), 4.3–5.8. BMI, GH, IGF-1, IGFBP-3 and HOMA-IR are described in the text

Table 2 Variables independently associated with NAFLD of stages 2–3

Variable	Univariate analysis		Multivariate analysis	
	P-value	RR (95% CI)	P-value	RR (95% CI)
AST	0.0235	0.238 (0.069–0.824)	0.0834	0.282 (0.067–1.182)
Platelet count	0.0181	4.667 (1.301–16.739)	0.0223	5.899 (1.288–27.017)
IGF-1	0.016	4.643 (1.331–16.196)	0.0363	4.568 (1.101–18.945)

The reference groups are AST ≤ 50 IU/l, platelet count < 200,000/l, and IGF-1 < 140 μg/l

Table 3 Correlation between serum hyaluronic acid and the GH/IGF-1/IGFBP-3 axis (n = 41)

Variable	Correlation coefficient	P-value
GH	0.135	NS
IGF-1	–0.427	0.0043
IGFBP-3	–0.352	0.0216
GH/IGF-1	0.338	0.0282
GH/IGFBP-3	0.175	NS
IGF-1/IGFBP-3	–0.436	0.0035

particularly strong negative correlation. As a reflection of these results, the GH/IGF-1 ratio, but not the GH/IGFBP-3 ratio, showed a positive correlation with the hyaluronic acid level, and similarly the IGF-1/IGFBP-3 ratio was positively correlated with hyaluronic acid.

Histopathology and the IGF-1 axis

Due to the negative correlation between IGF-1 and fibrosis, the relationships of IGF-1 with some aspects of

Brunt's fibrosis classification were evaluated. Patients were categorized based on the presence and absence of pericellular fibrosis, portal fibrosis, bridging fibrosis, and ballooning. No differences in IGF-1 were found for groups with and without pericellular fibrosis and bridging fibrosis, but IGF-1 was significantly lower in patients with portal fibrosis (stages 1–3) than in those without portal fibrosis ($P = 0.0229$), and the IGF-1/IGFBP-3 ratio showed a tendency to decrease in patients with portal fibrosis ($P = 0.0837$). In addition, the IGF-1 level was relatively low in patients showing ballooning ($P = 0.0816$) (Fig. 1). The relationship between histological grade of stages 0–1 or 2–3 was also examined, but no correlation was found.

Clinical and laboratory data in patients with steatosis of grade 1 and grades 2–3

The role of the GH/IGF-1/IGFBP-3 axis in steatosis was investigated by grouping patients into grades 1 and grades 2–3 using Brunt's steatosis classification (Table 4). There were no differences in sex, age, BMI, AST, ALT, γ-GTP, ALP, triglyceride, C-reactive protein, white blood cell count, red blood cell count, IGFBP-3, insulin, HOMA-IR score, and HbA1c between the two groups. However, total cholesterol ($P = 0.034$) and IGF-1 level ($P = 0.0180$) were higher in steatosis 2–3 patients and the GH level ($P = 0.0236$) was higher in steatosis 1 patients. In the multivariate analysis, a reduced GH level showed a significant association with steatosis of grades 2–3: GH (RR, 0.43; 95% CI, 0.002–0.772 [$P = 0.0328$]).

The results of univariate and multivariate analyses of risk factors for steatosis of grade 2–3 are shown in Table 5. In the univariate analysis, the following three factors were significantly associated with steatosis of grade 2–3: GH (RR, 0.196; 95% CI 0.046–0.830 [$P = 0.0269$]) and IGF (RR, 4.00; 95% CI, 1.151–13.901 [$P = 0.0291$]). In a multivariable analysis, GH (RR, 0.199; 95% CI, 0.042–0.989 [$P = 0.0414$]) was significantly associated with steatosis of grade 2–3.

Hepatic steatosis score and the GH axis

Correlations of hepatic steatosis score with GH, IGF-1, and IGFBP-3 levels were explored by examining differences in the GH/IGF-1, GH/IGFBP-3, and IGF-1/IGFBP-3 ratios between patients with steatosis of grade 1 and grades 2–3. The following factors showed a significant difference between these groups of patients: GH/IGF-1 ratio, $P = 0.0009$; GH/IGFBP-3 ratio, $P = 0.0019$ (Fig. 2), but IGF-1/IGFBP-3 ratio did not have any statistical difference.

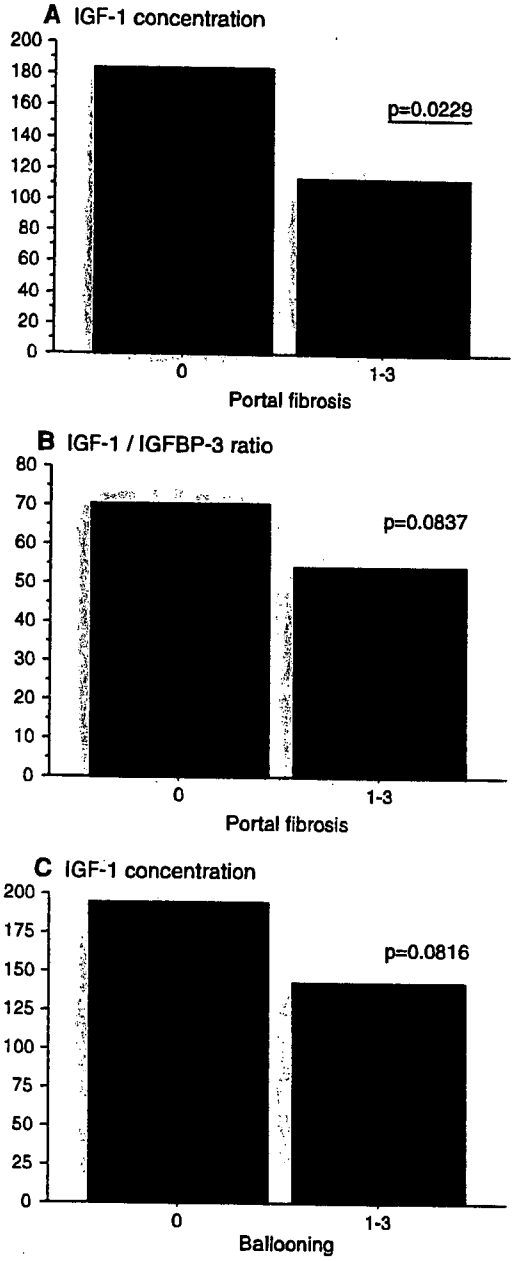

Fig. 1 Histopathologic factors and IGF-1: (A) relationship of portal fibrosis score and IGF-1 concentration (μg/l); (B) relationship of portal fibrosis score and IGF-1 concentration (μg/l)/IGFBP-3 concentration (mg/l) ratio; (C) relationship of ballooning score and IGF-1 concentration (μg/l). Statistical analysis by Mann–Whitney U test

Discussion

The data in this study shows that GH, IGF-1, and IGFBP-3 are predictors for the development of fibrosis and steatosis in NAFLD patients. Low levels of IGF-1 and IGF-1/IGFBP-3 may be associated with advanced fibrosis in NAFLD, and GH may be involved in the mechanism of

Table 4 Clinical and laboratory data for patients with steatosis of grade 1 and grades 2–3

Item	Steatosis 1 (n = 26)	Steatosis 2–3 (n = 26)	P-value
BMI	28.5 (4.48)	29.6 (3.75)	NS
Total cholesterol	193.7 (36.2)	211.4 (33.3)	0.034
Triglyceride	154.2 (65.6)	167.7 (66.6)	NS
GH	0.450 (0.458)	0.173 (0.162)	0.0236
IGF-1	157.1 (142.6)	184.3 (71.4)	0.0118
IGFBP-3	2.25 (0.58)	2.63 (0.68)	NS
Insulin	13.9 (5.89)	15.7 (7.83)	NS
Fasting plasma glucose	111.4 (28.2)	114.6 (38.2)	NS
HOMA-IR	4.02 (2.53)	4.04 (2.30)	NS
HbA1c	6.82 (1.75)	6.53 (2.08)	NS

Data are shown as means (standard deviation), with statistical analysis using a Mann–Whitney test

Table 5 Variables independently associated with steatosis of grade 2–3

Variable	Univariate analysis		Multivariate analysis	
	P-value	RR (95% CI)	P-value	RR (95% CI)
Total cholesterol	0.1239	2.424 (0.785–7.490)	0.3656	1.795 (0.506–6.372)
GH	0.0269	0.196 (0.046–0.830)	0.0414	0.199 (0.042–0.989)
IGF-1	0.0291	4.000 (1.151–13.901)	0.0676	3.628 (0.911–14.453)

The reference groups are total cholesterol > 200 mg/dl, GH > 0.3 ng/ml, and IGF-1 > 170 μg/l

triglyceride secretion from hepatocytes. It is of interest that our data are consistent with results of hormonal studies associated with atherosclerosis and metabolic syndrome [7, 9–11], and we speculate that the same hormonal profile results in development of hepatic steatosis and fibrosis in NAFLD, and that the mechanism of advanced fibrosis is common in development of atherosclerosis and visceral obesity.

Hepatic fibrosis is caused by activated hepatic stellate cells (HSC), which are activated by inflammatory cytokines in NAFLD [19]. Over expression of IGF-1 in HSC attenuates fibrogenesis and accelerates liver regeneration in a mouse model of CCl_4-induced liver damage [20]. These effects appear to be mediated in part by up-regulation of HGF and down-regulation of TGF-β1. Although GH is the major stimulant of IGF-1 synthesis in hepatocytes, inflammatory cytokines such as IL-1β [21], TNF-α [22] and IL-6 [23] inhibit IGF-1 secretion from hepatocytes. These cytokines are reported to have a pivotal role in development of NAFLD [24, 25], therefore, this may account for the decreased IGF-1 level and reduced IGF-1/IGFBP-3 ratio in advanced NASH and the negative correlation of these variables with the hyarulonic acid level. Based on the success of IGF-1 replacement therapy in animal models [26, 27], this therapy has recently been used for patients with liver cirrhosis [28]. IGF-1 supplementation protects the liver from damage, increases the albumin concentration and resting energy expenditure. The protective effects of IGF-1 on vascular cells, and endothelial function, atherosclerotic plaque development and ischemic myocardial damage all depend on nitric oxide production by activated PI3-k and Akt signaling in target cells [8]. IGF-1 induces glucose uptake in muscle [29] and low levels of IGF-1 produce different degrees of glucose tolerance in association with insulin sensitivity [30]; therefore, IGF-1 has been used successfully as an adjuvant to insulin therapy in patients with type 1 and 2 diabetes [29]. Insulin resistance is the most important factor in metabolic syndrome, including NAFLD and vascular disease, and low levels of IGF-1 may contribute to insulin resistance [29, 30]. IGF-1 has direct anti-fibrotic, cell protective and insulin-like actions and, decreases in IGF-1 and the IGF-1/IGFBP-3 ratio caused by inflammatory cytokines were associated with the development of advanced NAFLD, as well as serving as a marker for advanced NAFLD. In particular, our data show a tendency for low levels of IGF-1 and a low IGF-1/IGFBP-3 ratio in patients with portal fibrosis and ballooning. We speculate that this hormonal profile is required for progression of NAFLD, because of the emergence of portal fibrosis and ballooning in progressive NAFLD [31].

IGFBP-3 binds IGF-1 and an acid-labile subunit and forms a stable ternary complex, in which the half life of IGF-1 is prolonged and the bioactivity of IGF-1 is reduced [8]. New biological functions of IGFBP-3 have also been reported in recent years; for example, in mesangeal cells, IGFBP-3 mediates TNF-α and glucose-induced apoptosis by blocking Akt phosphorylation at threonine-308 [32].

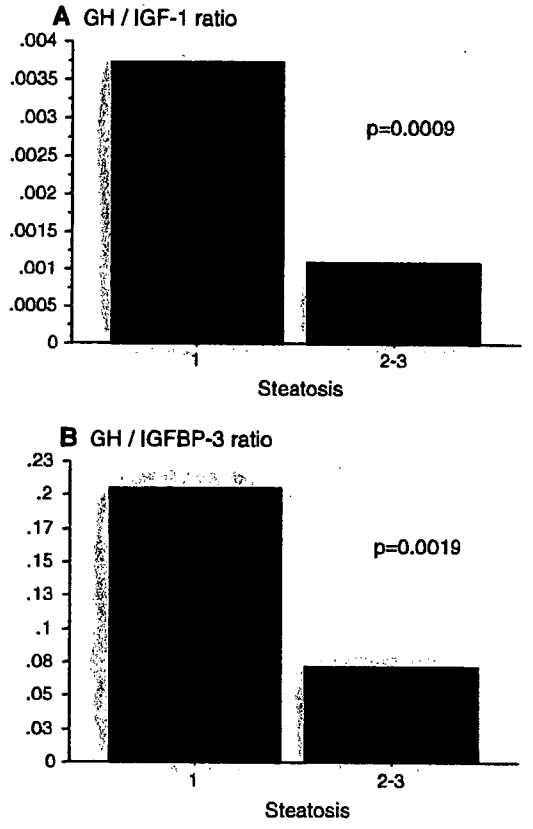

Fig. 2 Hepatic steatosis score and the GH axis: (A) relationship of steatosis score and GH (ng/ml)/IGF-1 concentration (μg/l) ratio; (B) relationship of steatosis score and GH (ng/ml)/IGFBP-1 concentration (mg/l) ratio. Statistical analysis by Mann–Whitney U test

Additionally, IGF-1 stimulates vascular endothelial growth factor (VEGF) and IGFBP-3 in retinal pigment epithelial cells, whereas, IGFBP-3 attenuates IGF-1-induced VEGF secretion [33]. IGF-1 also, inhibits TNF-α,(interferon γ and Fas-induced apoptosis in vascular smooth muscle cells, and TNF-α decreases IGF-1 and increases IGFBP-3 [22]. As stated above, IGFBP-3 binding reduces IGF-1 activity and the IGF-1/IGFBP-3 ratio therefore reflects the activity of IGF-1. In our study, hyaluronic acid, a hepatic fibrosis marker, showed negative correlations with IGF-1 ($r = -0.427$), IGFBP-3 ($r = -0.352$) and the IGF-1/IGFBP-3 ratio ($r = -0.436$). Although IGF-1 causes secretion of IGFBP-3 [6], we speculate that inflammatory cytokines decrease the levels of IGF-1 rather than those of IGFBP-3 in NAFLD patients, thereby decreasing the IGF-1/IGFBP-3 ratio. Therefore, a low IGF-1/IGFBP-3 ratio is a marker of advanced NAFLD, as it is for vascular disease.

The GH level did not show an association with fibrosis, but had a close affinity with steatosis in our cases. A low level of GH is the most reliable marker for advanced steatosis (grades 2–3], but the GH/IGF-1 and GH/IGFBP-3 ratios suggest that IGF-1 and IGFBP-3 are unrelated to steatosis. In previous reports, GH supplementation has been shown to reduce abdominal visceral fat in obese woman [34] and GHD patients [35], improve endothelial function in GHD patients [36], and decrease hepatic fat content in obese woman [34]. Such conditions are thought to promote GH-induced lipolysis in adipose tissue [37] and secretion of very low density lipoprotein from liver [38], and we suggest that low levels of GH may contribute to severe triglyceride accumulation in hepatocytes; though our results must be evaluated in a large cohort of patients.

In conclusion, GH, IGF-1 and IGFBP-3 are associated with fibrosis and steatosis of NAFLD. We speculate that a low level of IGF-1 and a low IGF-1/IGFBP-3 ratio may lead to development of fibrosis in NAFLD patients, whereas a low GH level contributes to development of hepatic steatosis. Since NAFLD is associated with metabolic syndrome, risk factors for development of these diseases show a common pattern of GH, IGF-1 and IGFBP-3 levels.

References

1. Johannsson G, Bengtsson BA. Growth hormone and the metabolic syndrome. J Endocrinol Invest 1999;22:41–6.
2. Ichikawa T, Hamasaki K, Ishikawa H, Ejima E, Eguchi K, Nakao K. Non-alcoholic steatohepatitis and hepatic steatosis in patients with adult onset growth hormone deficiency. Gut 2003;52:914.
3. Adams LA, Feldstein A, Lindor KD, Angulo P. Nonalcoholic fatty liver disease among patients with hypothalamic and pituitary dysfunction. Hepatology 2004;39:909–14.
4. Lonardo A, Loria P, Leonardi F, Ganazzi D, Carulli N. Growth hormone plasma levels in nonalcoholic fatty liver disease. Am J Gastroenterol 2002;97:1071–2.
5. Mauras N, Haymond MW. Are the metabolic effects of GH and IGF-I separable? Growth Horm IGF Res 2005;15:19–27.
6. Scharf J, Ramadori G, Braulke T, Hartmann H. Synthesis of insulin like growth factor binding proteins and of the acid-labile subunit in primary cultures of rat hepatocytes, of Kupffer cells, and in co-cultures: regulation by insulin, insulin like growth factor, and growth hormone. Hepatology 1996;23:818–27.
7. Juul A, Scheike T, Davidsen M, Gyllenborg J, Jorgensen T. Low serum insulin-like growth factor I is associated with increased risk of ischemic heart disease: a population-based case–control study. Circulation 2002;106:939–44.
8. Conti E, Carfozza C, Capoluongo E, Volpe M, Crea F, Zuppi C, Andreotti F. Insulin-like growth factor-1 as a vascular protective factor. Circulation 2004;110:2260–5.
9. Colao A, Spiezia S, Di Somma C, Pivonello R, Marzullo P, Rota F, Musella T, Auriemma RS, De Martino MC, Lombardi G. Circulating insulin-like growth factor-I levels are correlated with the atherosclerotic profile in healthy subjects independently of age. J Endocrinol Invest 2005;28:440–8.
10. Laughlin GA, Barrett-Connor E, Criqui MH, Kritz-Silverstein D. The prospective association of serum insulin-like growth factor I (IGF-I) and IGF-binding protein-1 levels with all cause and cardiovascular disease mortality in older adults: the Rancho Bernardo Study. J Clin Endocrinol Metab 2004;89:114–20.

11. Janssen JA, Stolk RP, Pols HA, Grobbee DE, Lamberts SW. Serum total IGF-I, free IGF-I, and IGFB-1 levels in an elderly population: relation to cardiovascular risk factors and disease. Arterioscler Thromb Vasc Biol 1998;18:277–82.
12. Adams LA, Lymp JF, St Sauver J, Sanderson SO, Lindor KD, Feldstein A, Angulo P. The natural history of nonalcoholic fatty liver disease: a population-based cohort study. Gastroenterology 2005;129:113–21.
13. Brea A, Mosquera D, Martin E, Arizti A, Cordero JL, Ros E. Nonalcoholic fatty liver disease is associated with carotid atherosclerosis: a case-control study. Arterioscler Thromb Vasc Biol 2005;25:1045–50.
14. Villanova N, Moscatiello S, Ramilli S, Bugianesi E, Magalotti D, Vanni E, Zoli M, Marchesini G. Endothelial dysfunction and cardiovascular risk profile in nonalcoholic fatty liver disease. Hepatology 2005;42:473–80.
15. Targher G. Associations between liver histology and early carotid atherosclerosis in subjects with nonalcoholic fatty liver disease. Hepatology 2005;42:974–5.
16. Brunt EM, Janney CG, Di Bisceglie AM, Neuschwander-Tetri BA, Bacon BR. Nonalcoholic steatohepatitis: a proposal for grading and staging the histological lesions. Am J Gastroenterol 1999;94:2467–74.
17. Taniguchi A, Fukushima M, Sakai M, Miwa K, Makita T, Nagata I, Nagasaka S, Doi K, Okumura T, Fukuda A, Kishimoto H, Fukuda T, Nakaishi S, Tokuyama K, Nakai Y. Remnant-like particle cholesterol, triglycerides, and insulin resistance in nonobese Japanese type 2 diabetic patients. Diabetes Care 2000;23:1766–9.
18. Zeng MD, Lu LG, Mao YM, Qiu DK, Li JQ, Wan MB, Chen CW, Wang JY, Cai X, Gao CF, Zhou XQ. Prediction of significant fibrosis in HBeAg-positive patients with chronic hepatitis B by a noninvasive model. Hepatology 2005;42:1437–45.
19. Elsharkawy AM, Oakley F, Mann DA. The role and regulation of hepatic stellate cell apoptosis in reversal of liver fibrosis. Apoptosis 2005;10:927–39.
20. Sanz S, Pucilowska JB, Liu S, Rodriguez-Ortigosa CM, Lund PK, Brenner DA, Fuller CR, Simmons JG, Pardo A, Martinez-Chantar ML, Fagin JA, Prieto J. Expression of insulin-like growth factor I by activated hepatic stellate cells reduces fibrogenesis and enhances regeneration after liver injury. Gut 2005;54:134–41.
21. Thissen JP, Verniers J. Inhibition by interleukin-1 beta and tumor necrosis factor-alpha of the insulin-like growth factor I messenger ribonucleic acid response to growth hormone in rat hepatocyte primary culture. Endocrinology 1997;138:1078–84.
22. Anwar A, Zahid AA, Scheidegger KJ, Brink M, Delafontaine P. Tumor necrosis factor-alpha regulates insulin-like growth factor-1 and insulin-like growth factor binding protein-3 expression in vascular smooth muscle. Circulation 2002;105:1220–5.
23. Lelbach A, Scharf JG, Ramadori G. Regulation of insulin-like growth factor-I and of insulin-like growth factor binding protein-1, -3 and -4 in cocultures of rat hepatocytes and Kupffer cells by interleukin-6. J Hepatol 2001;35:558–67.
24. Nozaki Y, Saibara T, Nemoto Y, Ono M, Akisawa N, Iwasaki S, Hayashi Y, Hiroi M, Enzan H, Onishi S. Polymorphisms of interleukin-1 beta and beta 3-adrenergic receptor in Japanese patients with nonalcoholic steatohepatitis. Alcohol Clin Exp Res 2004;28:106S–10S.
25. Larter CZ, Farrell GC. Insulin resistance, adiponectin, cytokines in NASH: which is the best target to treat? J Hepatol 2006;44:253–61.
26. Castilla-Cortazar I, Garcia M, Muguerza B, Quiroga J, Perez R, Santidrian S, Prieto J. Hepatoprotective effects of insulin-like growth factor I in rats with carbon tetrachloride-induced cirrhosis. Gastroenterology 1997;113:1682–91.
27. Garcia-Fernandez M, Castilla-Cortazar I, Diaz-Sanchez M, Navarro I, Puche JE, Castilla A, Casares AD, Clavijo E, Gonzalez-Baron S. Antioxidant effects of insulin-like growth factor-I (IGF-I) in rats with advanced liver cirrhosis. BMC Gastroenterol 2005;5:7.
28. Conchillo M, de Knegt RJ, Payeras M, Quiroga J, Sangro B, Herrero JI, Castilla-Cortazar I, Frystyk J, Flyvbjerg A, Yoshizawa C, Jansen PL, Scharschmidt B, Prieto J. Insulin-like growth factor I (IGF-I) replacement therapy increases albumin concentration in liver cirrhosis: results of a pilot randomized controlled clinical trial. J Hepatol 2005;43:630–6.
29. Dominici FP, Argentino DP, Munoz MC, Miquet JG, Sotelo AI, Turyn D. Influence of the crosstalk between growth hormone and insulin signalling on the modulation of insulin sensitivity. Growth Horm IGF Res 2005;15:324–36.
30. Sesti G, Sciacqua A, Cardellini M, Marini MA, Maio R, Vatrano M, Succurro E, Lauro R, Federici M, Perticone F. Plasma concentration of IGF-I is independently associated with insulin sensitivity in subjects with different degrees of glucose tolerance. Diabetes Care 2005;28:120–5.
31. Morita Y, Ueno T, Sasaki N, Kuhara K, Yoshioka S, Tateishi Y, Nagata E, Kage M, Sata M. Comparison of liver histology between patients with non-alcoholic steatohepatitis and patients with alcoholic steatohepatitis in Japan. Alcohol Clin Exp Res 2005;29:277S–81S.
32. Vasylyeva TL, Chen X, Ferry RJ Jr. Insulin-like growth factor binding protein-3 mediates cytokine-induced mesangial cell apoptosis. Growth Horm IGF Res 2005;15:207–14.
33. Slomiany MG, Rosenzweig SA. Autocrine effects of IGF-I-induced VEGF and IGFBP-3 secretion in retinal pigment epithelial cell line ARPE-19. Am J Physiol Cell Physiol 2004; 287:C746–53.
34. Franco C, Brandberg J, Lonn L, Andersson B, Bengtsson BA, Johannsson G. Growth hormone treatment reduces abdominal visceral fat in postmenopausal women with abdominal obesity: a 12-month placebo-controlled trial. J Clin Endocrinol Metab 2005;90:1466–74.
35. Eden Engstrom B, Burman P, Holdstock C, Karlsson FA. Effects of growth hormone (GH) on ghrelin, leptin, and adiponectin in GH-deficient patients. J Clin Endocrinol Metab 2003;88:5193–8.
36. Abdu TA, Elhadd TA, Buch H, Barton D, Neary R, Clayton RN. Recombinant GH replacement in hypopituitary adults improves endothelial cell function and reduces calculated absolute and relative coronary risk. Clin Endocrinol (Oxf) 2004;61:387–93.
37. Kersten S. Mechanisms of nutritional and hormonal regulation of lipogenesis, EMBO Rep 2001;2:282–6.
38. Frick F, Linden D, Ameen C, Eden S, Mode A, Oscarsson J. Interaction between growth hormone and insulin in the regulation of lipoprotein metabolism in the rat. Am J Physiol Endocrinol Metab 2002;283:E1023–31.

ELSEVIER

Cerebellar Ataxia in a Patient Receiving Calcineurin Inhibitors After Living Donor Liver Transplantation: A Case Report

I. Yamaguchi, T. Ichikawa, K. Nakao, K. Hamasaki, K. Hirano, S. Eguchi, M. Takatsuki, Y. Kawasita, T. Kanematsu, and K. Eguchi

ABSTRACT

Neurological complications of calcineurin inhibitors are frequent problems after transplantation. Cerebellar ataxia with other neurological findings and an abnormal density area in the subcortical white matter are found by MRI in the brains of most patients with central nervous system complications caused by calcineurin inhibitors. Such neurological complications are not life-threatening, but have a negative impact on the quality of life. We describe a 58-year-old woman who developed cerebellar ataxia at 4 days after living donor liver transplantation. She walked with a swaying gait, and after walking for 5 minutes she was unable to stand. Her symptoms persisted after a change from tacrolimus to cyclosporine, but dose reduction of cyclosporine and addition of mycophenolate mofetil cured the ataxia. We diagnosed a case of cerebellar ataxia without leukoencephalopathy or other neurological symptoms, as a new complication of calcineurin inhibitor treatment. We concluded that careful attention should be paid to neurological complications of calcineurin inhibitors.

TACROLIMUS (Tac) and cyclosporine (CsA) are calcineurin inhibitors that have powerful immunosuppressant actions, which may lead to adverse neurological effects postoperatively in organ transplant patients. In a previous report,[1] calcineurin inhibitors were shown to cause various neurotoxic events, including seizures, tremors, changes in mental state, peripheral neuropathy, and leukoencephalopathy among 10% to 28% of treated patients. Most patients suffered leukoencephalopathy. Herein, we have reported a case of a patient who received a living donor liver transplantation (LDLT) and subsequently developed cerebellar ataxia which manifested as gait and speech disturbances. This complication resolved following reduction of the calcineurin inhibitor dose. This case differs from previously reported cases regarding neurological symptoms and brain MRI findings.

CASE REPORT

A 58-year-old woman with hepatitis C virus (HCV; genotype 1b and 2140 fmol/L serum core protein) and decompensated liver cirrhosis underwent LDLT. Before LDLT, she had experienced hepatic encephalopathy, but did not have any other neurological complication. After LDLT, Tac and prednisone were administered at the standard doses used in our immunosuppressive protocol. On postoperative day (POD) 7, she had slurred speech and intention tremor, but these occurred without seizure, muscle weakness, or any other neurological symptoms except for cerebellar ataxia. Her gait posture had a wide base, she swayed while walking, and she could barely walk for 5 minutes before becoming unstable. She could not stand on one foot and or step in tandem gait. We thought that her neurological condition was due to cerebellar ataxia caused by Tac.

On POD 23, laboratory data showed 1100 fmol/L HCV virus titer, 754 IU/mL alanine aminotransferase (ALT) 853 IU/mL alkaline phosphatase (ALP), and 3.0 mg/dL total bilirubin. We diagnosed reactivation of HCV based on the laboratory data and a liver biopsy, and started interferon (IFN) α-2b at 3 million units subcutaneously 3 times per week plus ribavirin (Rib) at 400 mg/d orally for 24 weeks. Because of the persistence of her neurological symptoms, Tac was discontinued and CsA was started from POD 22. At the end of the IFN plus Rib therapy, HCV remained in her serum. Therefore, she resumed pegylated IFN (peg-IFN) α-2b (60 μg subcutaneously once per week) plus Rib (600 mg/d orally for 24 weeks) from postoperative week 38. Within the period of peg-IFN α-2b plus Rib treatment, the serum HCV virus titer decreased but

From the First Department of Internal Medicine (I.Y., T.I., K.N., K.H., K.E.) and Departments of Clinical pharmaceutics (K.H.) and Transplantation and Digestive Surgery (S.E., M.T., Y.K., T.K.), Graduate School of Biomedical Science, Nagasaki University, Nagasaki, Japan.

Address reprint requests to Tatsuki Ichikawa, MD, First Department of Internal Medicine, Graduate School of Biomedical Science, Nagasaki University, 1-7-1 Sakamoto, Nagasaki, Japan. E-mail: ichikawa@net.nagasaki-u.ac.jp

0041-1345/07/$–see front matter
doi:10.1016/j.transproceed.2007.08.092

her laboratory data did not normalize and she experienced an auditory disturbance in her right ear due to adverse effects of IFN treatment. On MRI on POD 48, no abnormal intensity regions were found in the deep white matter in the cerebrum and cerebellum. Because cerebellar ataxia persisted after the change from Tac to CsA, she tended to fall down easily and her independent range of movement was restricted. At postoperative month 13, peg-IFN α-2b plus Rib therapy was terminated at the cutoff date for this therapy. After cessation of IFN combination therapy, her laboratory data worsened and the serum HCV virus titer was elevated. The hearing disturbance subsided, but the neurological symptoms due to cerebellar ataxia continued. We determined that retreatment with IFN plus Rib was needed to repress liver fibrosis. On POD 464, the patient undertook a new immunosuppressive regimen including CsA, which was reduced from 200 to 100 mg/d, and mycophenolate mofetil (MMF), 1 g/d. The next day, cerebellar ataxia improved and she could walk for 20 minutes or more. The blood CsA concentration fell below therapeutic range, 48 ng/mL, after reduction of the CsA dose. Two months after reduction of CsA, the patient was not conscious of cerebellar ataxia, since her independent activities were no longer restricted, and she did not have intention tremor, or the inability to step in tandem gait or stand on one foot. In this context, peg-IFN α2a (180 μg once per week) and Rib (400 mg daily for 48 weeks) had been started from POD 452, and the HCV titer decreased from 71,400 fmol/L to below the detection limit in the HCV core protein assay. Similarly, ALT decreased from 192 to 50 IU/mL in the 2 months after the start of the new anti-HCV regimen. Follow-up brain MRI was performed at the termination of the new anti-HCV regimen; no abnormal intensity area was found in the brain. The patient no longer noticed hearing disturbances during this period, despite the repeated IFN treatment.

DISCUSSION

Liver transplantation is now a well-established treatment for end-stage liver disease. The quality of life after liver transplantation is excellent in most patients, but some patients suffer complications, many of which are related to the immunosuppressive therapy.[2] Neurological complications are common adverse effects of immunosuppressants, and calcineurin inhibitors are known for their neurotoxicity. The majority of neurological complications are not life-threatening,[3] but lead to an impaired quality of life. In our case, cerebellar ataxia decreased the activities of our patient, and a calcineurin inhibitor sparing regimen improved her lifestyle following amelioration of cerebellar ataxia. Our experience suggested that greater consideration of neurological complications caused by adverse effects of calcineurin inhibitors is warranted, because impaired quality of life caused by postoperative neurological complications can be improved by dose reduction of calcineurin inhibitors.[1]

In most cases, central nervous system complications caused by CsA involve lesions with increased signal intensity on MRI T2-weighted images, with these lesions affecting the subcortical white matter.[4] In other reports, cerebrocerebellar syndrome,[3] cerebellar syndrome,[5] mutism with ataxia,[6] loss of speech with ataxia,[7] and late-onset ataxia[8] have been associated with high signal intensity regions in the white matter on MRI T2-weighted images. Such high signal intensity in the white matter on MRI is referred to as leukoencephalopathy, a well-known clinical aspect of various types of toxic encephalopathy, including that due to calcineurin inhibitors.[9] In contrast, ataxia without abnormal MRI findings represents a rare form of neurological complication following liver transplantation.[3] Leukoencephalopathy was not found in the subcortical white matter in our case, but we consider that the case was still a toxic complication of a calcineurin inhibitor, because of the improved ataxia upon reduction of the CsA dose. Therefore, we assume that the neurological complications were also adverse effects of the calcineurin inhibitor, despite the absence of MRI findings. The mechanisms of neurological toxicity without leukoencephalopathy are not well understood. In vitro experiments[1] have shown that Tac and CsA have selective toxicity for glial cells and induce apoptosis of oligodendrocytes. It is speculated that these events correlate with typical white matter changes. However, Tac and CsA may modulate the activity of amino acid receptors via calcineurin in neurons.[1] This phenomenon may cause alteration of neuronal function and development of neurological complications without morphological changes in the brain. Hence, it is possible that a patient with neurological complications caused by calcineurin inhibitors could show normal deep white matter on MRI.

Although the neurological symptoms in our case were of the early-onset posttransplantation type, as in other reports,[1] ataxia without other neurological symptoms is rare in a patient receiving a calcineurin inhibitor. Previously reported patients with neurological complications who were treated with Tac and CsA almost always had ataxia plus other neurological symptoms, such as muscle weakness[7] or blindness and seizure.[3] Ataxia alone has been reported in a late-onset case of neurological complications induced by a calcineurin inhibitor,[10] and the cerebellum has been reported to be affected in a few cases.[11] However, the mechanism of cerebellum neurotoxicity remains unknown, and it is more likely that the cerebellar hemisphere alone is damaged by calcineurin inhibitors. Calcineurin plays a pivotal role in cerebellar development,[12] and the calcineurin signal may contribute to the maturation and refinement of cerebellar circuit formation.[12] Therefore, we suggest that a calcineurin inhibitor can have a functional influence on the cerebellum without causing morphological changes.

Central nervous system involvement in HCV infection with or without cryoglobulinemia has been reported previously.[13] Therefore, it is a key issue whether calcineurin inhibitors were more relevant to the neurological symptoms of this case rather than reactivation of HCV infection after LDLT. As described in the clinical course, HCV activity decreased during the therapy with IFN or peg-IFN plus Rib and increased after cessation of therapy. Cerebellar ataxia persisted independently of HCV activity, but improved after dose reduction of CsA. Taken together, it is possible that calcineurin inhibitors rather than HCV activity were

directly related to cerebellar ataxia. However, HCV reactivation after LDLT may be, at least in part, a triggering factor for the neurological deficient in this case as discussed previously.[14]

In conclusion, we have proposed that cerebellar ataxia without other neurological findings is a new adverse event associated with calcineurin inhibitors. This condition was shown not to involve leukoencephalopathy using MRI. Ataxia caused a significant negative impact on the daily life of our patient. Reduction of the calcineurin inhibitor dose reversed her condition, but the change from Tac to CsA was not effective. Hence, it is important to determine whether neurologically adverse effects in transplanted patients originate from calcineurin inhibitors, and familiarity with the side effects of calcineurin inhibitors is important when using these agents.

REFERENCES

1. Bechstein WO: Neurotoxicity of calcineurin inhibitors: impact and clinical management. Transpl Int 13:313, 2000

2. Compston JE: Osteoporosis after liver transplantation. Liver Transpl 9:321, 2003

3. Stein DP, Lederman RJ, Vogt DP, et al: Neurological complications following liver transplantation. Ann Neurol 31:644, 1992

4. Sheth TN, Ichise M, Kucharczyk W: Brain perfusion imaging in asymptomatic patients receiving cyclosporin. Am J Neuroradiol 20:853, 1999

5. Vogt DP, Lederman RJ, Carey WD, et al: Neurologic complications of liver transplantation. Transplantation 45:1057, 1988

6. Sokol DK, Molleston JP, Filo RS, et al: Tacrolimus (FK 506)-induced mutism after liver transplant. Pediatr Neurol 28:156, 2003

7. Bronster DJ, Boccagni P, O'Rourke M, et al: Loss of speech after orthotopic liver transplantation. Transpl Int 8:234, 1995

8. Garcia-Escrig M, Martinez J, Fernandez-Ponsati J, et al: Severe central nervous system toxicity after chronic treatment with cyclosporine. Clin Neuropharmacol 17:298, 1994

9. Hinchey J, Chaves C, Appignani B, et al: A reversible posterior leukoencephalopathy syndrome. N Engl J Med 334:494, 1996

10. Belli LS, De Carlis L, Romani F, et al: Dysarthria and cerebellar ataxia: late occurrence of severe neurotoxicity in a liver transplant recipient. Transpl Int 6:176, 1993

11. Nussbaum ES, Maxwell RE, Bitterman PB, et al: Cyclosporine A toxicity presenting with acute cerebellar edema and brainstem compression. Case report. J Neurosurg 82:1068, 1995

12. Sato M, Suzuki K, Yamazaki H, et al: A pivotal role of calcineurin signaling in development and maturation of postnatal cerebellar granule cells. Proc Natl Acad Sci USA 102:5874, 2005

13. Filippini D, Colombo F, Jann S, et al: Central nervous system involvement in patients with HCV-related cryoglobulinemia: literature review and a case report. Reumatismo 54:150, 2002

14. Belli LS, De Carlis L, Romani F, et al: Dysarthria and cerebellar ataxia: late occurrence of severe neurotoxicity in a liver transplant recipient. Transpl Int 6:176, 1993

X-linked inhibitor of apoptosis (XIAP) and XIAP-associated factor-1 expressions and their relationship to apoptosis in human hepatocellular carcinoma and non-cancerous liver tissues

RYOSUKE SAKEMI[1-3], HIROHISA YANO[1,3], SACHIKO OGASAWARA[1,3], JUN AKIBA[1,3], OSAMU NAKASHIMA[1,3], SUGURU FUKAHORI[1,3], MICHIO SATA[2,3] and MASAMICHI KOJIRO[1,3]

[1]Department of Pathology and [2]Division of Gastroenterology, Department of Medicine, Kurume University School of Medicine; [3]Research Center of Innovative Cancer Therapy of the 21st Century COE Program for Medical Science, Kurume University, Kurume, Fukuoka 830-0011, Japan

Received March 1, 2007; Accepted April 2, 2007

Abstract. The X-linked inhibitor of apoptosis (XIAP) belongs to the inhibitor of apoptosis (IAP) family, and the action of XIAP is inhibited by XIAP-associated factor-1 (XAF1). In the present study, XIAP and XAF1 protein expressions and their relationship to apoptosis were investigated in hepatocellular carcinoma (HCC). We examined immunohistochemical expressions of XIAP and XAF1, and the number of apoptotic HCC cells in surgically resected tissues of 24 HCCs, consisting of 7 well-, 10 moderately and 7 poorly differentiated HCCs. As a result, XIAP and XAF1 expressions were identified in the cytoplasm of non-neoplastic and neoplastic hepatocytes. In the 24 HCCs, XIAP expression was not different according to the histological grade of HCC. In contrast, XAF1 expression was significantly lower in poorly differentiated than that in well- or moderately differentiated HCCs (P=0.001), or XIAP expression in poorly differentiated HCC (P<0.001). Apoptotic HCC cell number was significantly lower in poorly differentiated than that in well- or moderately differentiated HCCs (P<0.01). A significant relationship was observed between XAF1 expression and apoptotic cell number in HCC tissues. In conclusion, the present findings suggest that significantly low XAF1 expression, but not XIAP expression, in poorly differentiated HCC may relate to resistance to apoptosis.

Introduction

Apoptosis is an active process of gene-directed cellular self-destruction and is observed in the sculpting of organs and tissues during embryonic development and the removal of old unnecessary cells for the maintenance of tissue homeostasis. Apoptosis is also observed in some pathological processes, such as in the elimination of tumor cells and virus-infected cells, and thereby contributes to the self-defense mechanisms. In the process of apoptosis, activation of the caspase family, especially caspase-3, plays an important role (1-3).

The inhibitor of apoptosis (IAP) family contains intrinsic cellular regulators of apoptosis and includes X-linked IAP (XIAP), c-IAP1, c-IAP2, NAIP, ML-IAP, ILP-2, survivin and Apollon (4). These proteins are characterized by the presence of one to 3 copies of a ~70-amino acid domain termed the baculoviral inhibitory repeat (BIR) at the amino terminus of the protein. The BIR domains have been shown to bind and inhibit caspase-3, -7, and -9 (4-6). Among the IAP family, XIAP protein contains 3 copies of the BIR domain and one RING domain at the extreme carboxyl terminus of the protein. *In vitro* kinetic studies have shown that XIAP is the most potent caspase inhibitor and suppressor of apoptosis in the IAP family (4,6). Various levels of XIAP mRNA and protein were expressed in human cancer cell lines (7,8), suggesting the involvement of XIAP in the apoptosis resistance mechanism of cancer cells.

The caspase-inhibiting activity of XIAP is negatively regulated by at least two XIAP-interacting proteins, XIAP-associated factor-1 (XAF1) (8,9) and Smac/DIABLO (10,11). XAF1, a 34-kDa zinc finger protein, was identified in a yeast two-hybrid screen based on its ability to bind XIAP and was found to antagonize the ability of XIAP to suppress caspase activity and cell death *in vitro* (6). XAF1, which resides in the nucleus, can effect a relocalization of XIAP from the cytoplasm to nucleus and neutralize XIAP's ability to inhibit apoptosis (9). Smac/DIABLO, which is localized in mitochondria, is released into cytoplasm and processed into an active form during mitochondria-induced apoptosis (10,11). The binding of active Smac/DIABLO to XIAP is proposed to destabilize the XIAP-caspase interaction by steric hindrance, resulting in disruption of the XIAP-caspase complex (12,13). XAF1 is ubiquitously expressed in normal tissues, but is present at very low or undetectable levels in many cancer cell lines (8,9). Byun *et al* (14) found that a substantial fraction of gastric cancer cell lines and tissues express no or extremely low levels

Correspondence to: Dr Hirohisa Yano, Department of Pathology, Kurume University School of Medicine, 67 Asahi-machi, Kurume, Fukuoka 830-0011, Japan
E-mail: hiroyano@med.kurume-u.ac.jp

Key words: apoptosis, hepatocellular carcinoma, XIAP-associated factor-1, X-linked inhibitor of apoptosis

of the XAF1 transcript, whereas Smac/DIABLO was normally expressed in all cancer specimens.

Hepatocellular carcinoma (HCC) often develops in patients with hepatitis B or C virus-related chronic hepatitis or liver cirrhosis. In non-HCC tissues, apoptosis of hepatocytes, showing chromatin condensation of the nuclei and eosinophilic change of the cytoplasm, is often observed, and the number of such apoptotic cells is in proportion to inflammatory activity. On the other hand, abnormalities in the expression of apoptosis-related molecules, and the resistance to various apoptosis-inducing stimuli have been reported in HCC (15,16). Except for the study of Shiraki *et al* (17) who examined XIAP expression in HCC tissues, there have been no comparative studies on XAF1 and XIAP expressions according to the histological grade, and no study to explore the relationship between the frequency of apoptosis and XAF1 or XIAP expression in human HCC tissues. These are addressed in the present study.

Materials and methods

Tissue samples. Immunohistochemical examination was performed on formalin-fixed, paraffin-embedded sections of cancerous and non-cancerous tissues obtained from 24 surgically resected HCCs at the Kurume University Hospital between 1989 and 2003. The 24 patients ranged from 50 to 84 years of age, and consisted of 18 males and 6 females. Two were serum hepatitis B surface antigen-positive, 19 were positive to the hepatitis C virus antibody, and the remaining 3 patients were not positive to either. The 24 cases did not receive preoperative anticancer therapies such as transcatheter arterial embolization (TAE) and percutaneous ethanol injection therapy. Among the 24 cases, seven had well-differentiated HCC, 10 had moderately differentiated HCC, and 7 had poorly differentiated HCC. The non-HCC tissues showed liver cirrhosis in ten cases and chronic hepatitis in 14. Informed consent was obtained from all patients included in the study.

Immunohistochemistry. Formalin-fixed, paraffin-embedded serial sections (4 μm) were mounted on 3-aminopropyltriethoxysilane-coated slides (Matsunami Glass Ind., Ltd., Osaka, Japan), and deparaffinized in xylene alcohol and graded alcohol. For XIAP immunostaining, the sections were soaked in 10 mmol/l of sodium citrate buffer (pH 6.9) and treated in a microwave for 30 min for antigen retrieval. XIAP and XAF1 expressions were immunohistochemically examined with mouse monoclonal anti-XIAP antibody (3.0 μg/ml, BD Biosciences, San Jose, CA) and rabbit polyclonal anti-XAF1 antibody (4 μg/ml, IMGENEX, San Diego, CA) as the primary antibodies, and using catalyzed signal-amplification system II (Code K1497, Dako, Ely, UK) according to the manufacturer's protocol. The sections for XIAP immunostaining were incubated with primary antibody for 60 min at room temperature after blocking endogenous biotin and peroxidase activities, and the sections for XAF1 were incubated overnight with primary antibodies at 4°C. Negative controls were prepared by replacing the primary antibody with normal mouse IgG or normal rabbit IgG. The peroxidase reaction was developed with the addition of 3,3-diaminobenzidine and H_2O_2 substrate solution. After counterstaining with hematoxylin, the slides were dehydrated, coverslipped, and observed under a microscope (Olympus BH-2, Olympus Optical, Tokyo, Japan).

Evaluation of immunohistochemical findings. The results of immunohistochemistry were evaluated according to the rate of staining and grading of expression by two pathologists (Y.S. and H.Y.). XIAP and XAF1 expressions in non-HCC tissues are relatively homogeneous and were used as an internal positive control. Regarding XIAP and XAF1, an expression score system was assigned on the basis of multiplying the rate of cells staining positive by the intensity of staining. The staining intensity was scored on a scale from 0 to 2 (0, HCC cells with no positive reactions; 0.5, HCC cells stained less intensely than hepatocytes; 1.0, HCC cells stained as intensely as hepatocytes; 2.0, HCC cells more intensely stained than hepatocytes). The final score was calculated as the sum of each staining intensity multiplied by the rate of the corresponding area. For example: if a HCC nodule shows 30% HCC cells stained less intensely than hepatocytes, 50% HCC cells stained as intensely as hepatocytes, and 20% HCC cells more intensely stained than hepatocytes, the score would be (0.3x0.5) + (0.5x1.0) + (0.2x2.0) = 1.05.

Assessment of number of apoptosic cells in HCC tissues. The number of cells showing the characteristics of apoptosis (e.g., cytoplasmic shrinkage, chromatin condensation and nuclear fragmentation) was counted in 14-25 0.25 mm^2-areas within HCC nodules stained with hematoxylin-eosin (HE).

Statistics. Group differences were obtained for the expression score of XIAP and XAF1, and apoptosis number with the Mann-Whitney test. The correlation between the number of apoptosic cells and the expression of XIAP or XAF1 was examined by Pearson's correlation coefficient. All statistical analyses were performed with StatMate III (ATMS Co., Ltd., Tokyo, Japan). P-values <0.05 were considered significant.

Results

XIAP and XAF1 expressions in HCC and non-HCC tissues. In non-HCC tissue, XIAP was expressed in the cytoplasm of hepatocytes, and the XIAP-expressing cells were relatively homogeneously distributed in the liver lobule (Fig. 1A and B). XAF1 was also expressed in the cytoplasm of hepatocytes. The XAF1-expressing cells were almost homogeneously distributed, but the more strongly expressing cells were scattered in the areas around portal tracts with marked cellular infiltration (Fig. 1C). Cirrhosis and chronic hepatis did not differ in the intensity or distribution of XAF1 expression. Negative controls showed no staining for XIAP or XAF1 (data not shown).

In HCC tissue, XIAP was expressed in the cytoplasm of HCC cells, and the XIAP-expressing cells in cancer nodules were more homogeneously distributed than the XAF1-expressing cells (Fig. 2A and B). XAF1 was also expressed in the cytoplasm of HCC cells. However, the XAF1 expression levels in well- and moderately differentiated HCC nodules varied with individual cancer cells, showing a heterogeneous distribution. In particular, XAF1 expression was conspicuous in HCC cells with fatty change and immediately subcapsular HCC cells in the periphery of cancer nodules (Fig. 2A and B; Fig. 3).

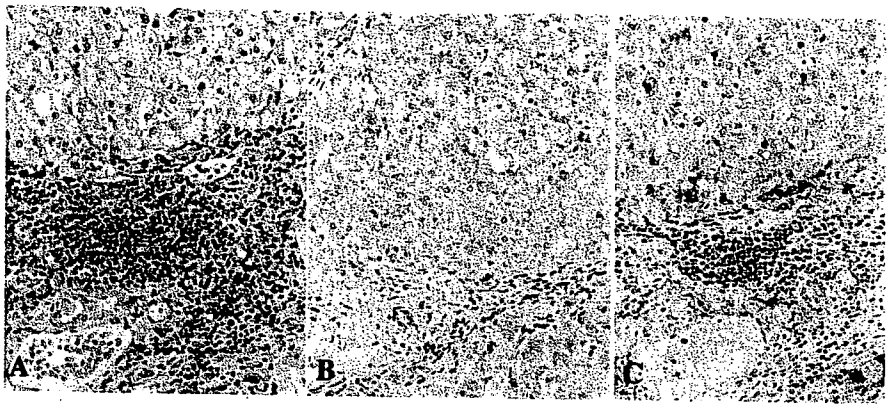

Figure 1. (A) Photomicrograph showing a portal area with active infiltration of lymphocytes, and periportal non-neoplastic hepatocytes (hematoxylin-eosin stain, x100). (B) Immunohistochemical staining for XIAP showing homogeneous expression in hepatocytes (counterstained with Mayer's hematoxylin, x100). (C) Immunohistochemical staining for XAF1 showing homogeneous expression in hepatocytes, except in those around the portal areas with active infiltration of inflammatory cells, which showed strong expression (counterstained with Mayer's hematoxylin, x100).

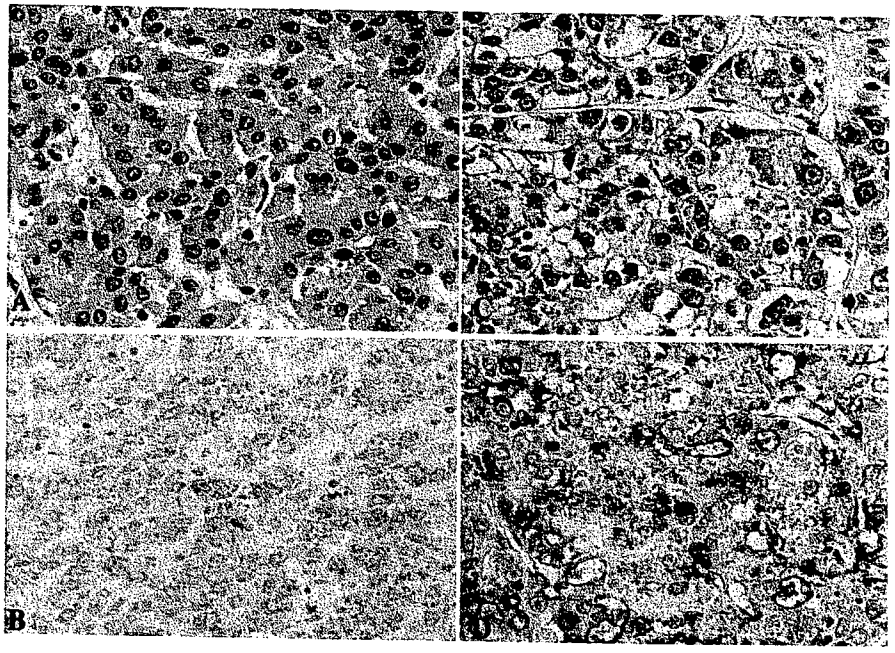

Figure 2. (A) Photomicrograph showing moderately differentiated hepatocellular carcinoma (HCC) with a thick trabecular arrangement (hematoxylin-eosin stain, x200). (B) Immunohistochemical staining for XIAP showing homogeneous expression in HCC cells (counterstained with Mayer's hematoxylin, x200). (C) Photomicrograph showing moderately differentiated HCC with fatty change and a relatively compact arrangement (hematoxylin-eosin stain, x200). (D) Immunohistochemical staining for XAF1 showing strong expression in HCC cells with fatty change (counterstained with Mayer's hematoxylin, x200).

The numbers of well-, moderately and poorly differentiated HCCs with an XIAP expression score of 1 or higher were 5 (71%), 5 (50%) and 6 (86%), respectively. The XIAP expression scores in the well-, moderately and poorly differentiated HCCs were 1.07±0.44 (mean ± SD), 1.10±0.69 and 1.17±0.38, respectively, showing no significant differentiation-dependent differences [Fig. 4 (left panel)]. The numbers of well-, moderately and poorly differentiated HCCs with an XAF1 expression score of 1 or higher were 6 (86%), 6 (60%) and 0 (0%), respectively. The XAF1 expression scores in the well-, moderately and poorly differentiated HCCs were 1.14±0.54 (mean ± SD), 1.14±0.47 and 0.19±0.16, respectively, indicating that the expression was significantly lower in the poorly differentiated HCCs than in the well- and moderately differentiated HCCs [P<0.001, Fig. 4 (left panel)]. In the poorly differentiated HCCs, the expression score of XAF1 was significantly lower than that of XIAP [P<0.001, Fig. 4 (right panel)]. No other differentiation-dependent differences were noted between the expression scores of XIAP and XAF1.

Presence of apoptosis and its relationship to XIAP and XAF1 expression in HCC. Fig. 5A shows typical apoptotic tumor cells (arrows) in moderately differentiated HCC tissue. The numbers of apoptotic cells per area in well-, moderately and poorly differentiated HCC nodules were 3.55±1.86 (mean ± SD), 3.62±1.46 and 1.76±0.46, respectively, indicating that the number of apoptotic cells was significantly smaller in the poorly differentiated than in the well- and moderately differentiated HCCs (P<0.01, Fig. 5B). In the 24 HCCs, the number of apoptotic cells per area was significantly correlated with XAF1 expression, but not with XIAP expression (Fig. 6).

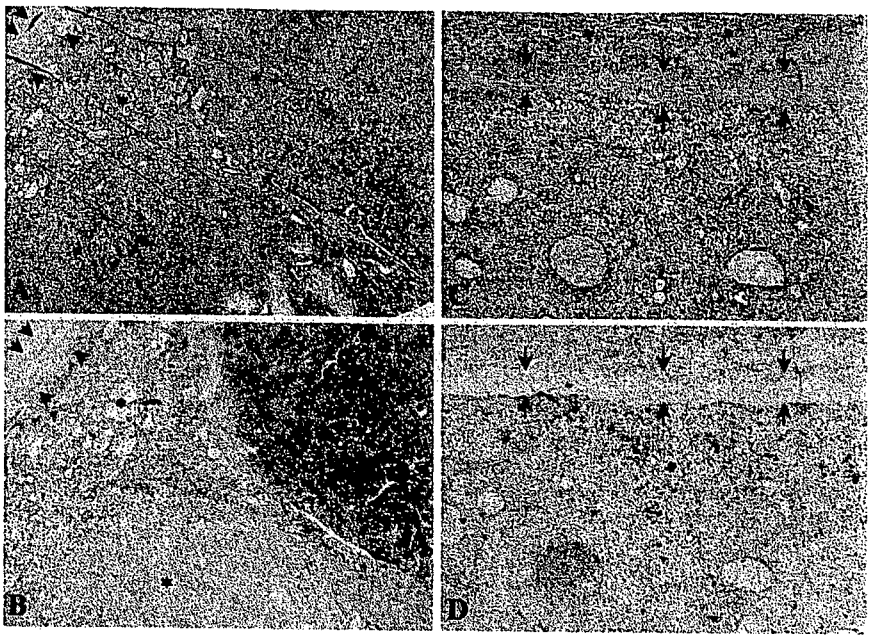

Figure 3. (A) Photomicrograph showing a hepatocellular carcinoma (HCC) nodule with a fibrous capsule (arrows). The nodule contains areas of moderately differentiated HCC with a trabecular arrangement (*), that with a pseudoglandular arrangement (•), and that with fatty change (Δ) (hematoxylin-eosin stain, x5). (B) Immunohistochemical staining for XAF1 showing heterogeneous expression. Upper right areas of moderately differentiated HCC with fatty change (Δ) and surrounding moderately differentiated HCC show strong expression, whereas the other areas show low levels of expression (counterstained with Mayer's hematoxylin, x5). (C) Photomicrograph showing a HCC nodule with a fibrous capsule (arrows) surrounded by non-HCC tissues (•) (hematoxylin-eosin stain, x20). (D) Immunohistochemical staining for XAF1 showing that HCC cells near the capsule (arrows) tend to show stronger XAF1 expression (counterstained with Mayer's hematoxylin, x20).

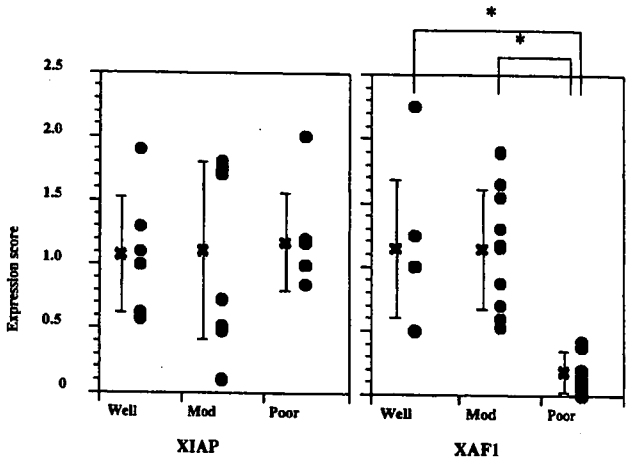

Figure 4. (Left panel) Expression scores of XIAP and XAF1 according to the histological grade of hepatocellular carcinoma (HCC). (Right panel) Comparison of expression scores between XIAP and XAF1 in poorly differentiated HCC. Data represent the mean ± SD (n=7-10). Well, well-differentiated HCC; mod, moderately differentiated HCC; poor, poorly differentiated HCC. *P<0.001 by the Mann-Whitney test.

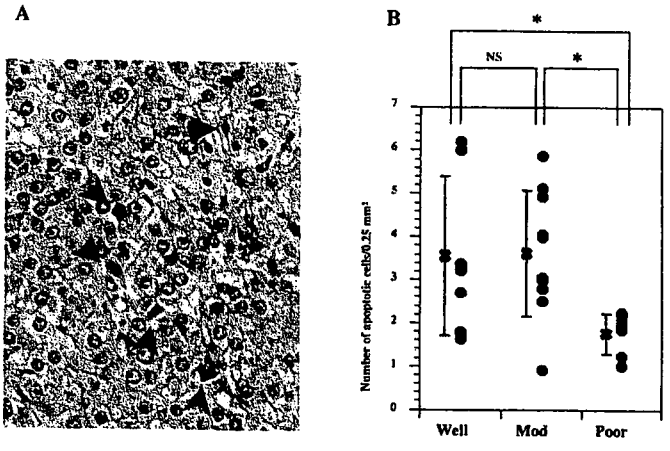

Figure 5. (A) Photomicrograph showing typical apoptotic tumor cells (arrows) with eosinophilic shrunken cytoplasm and pyknotic nuclei in moderately differentiated hepatocellular carcinoma (HCC) tissue (hematoxylin-eosin stain, x400). (B) Number of apoptotic HCC cells according to the histological grade. Data represent the mean ± SD (n=7-10). Well, well-differentiated HCC; mod, moderately differentiated HCC; poor, poorly differentiated HCC; NS, not significant. *P<0.01 by the Mann-Whitney U test.

Discussion

A recent immunohistochemical study revealed that the expression of XIAP protein in normal human tissues was heterogeneous and showed a higher selectivity to particular cell types (18). The expression of XIAP has also been confirmed in various tumor cell lines by Western blot analysis (7) and in various malignant neoplastic tissues, including non-small cell lung cancer, cervical carcinoma, prostate carcinoma and esophageal squamous cell carcinoma by immunohistochemistry, in which a higher expression was observed compared with normal counterparts (reviewed in ref. 18). These results suggest that overexpression of XIAP may contribute to resistance to apoptosis in various types of cancer cells. Studies using immunostaining have reported that XIAP protein is absent or weakly expressed in normal liver and the non-cancerous tissue of HCC (17,18). In contrast, Shiraki *et al* (17) reported that 14 of 20 (70%) HCC tissue samples demonstrated moderate or strong cytoplasmic staining for XIAP, and that XIAP expression was inversely correlated with apoptosis in

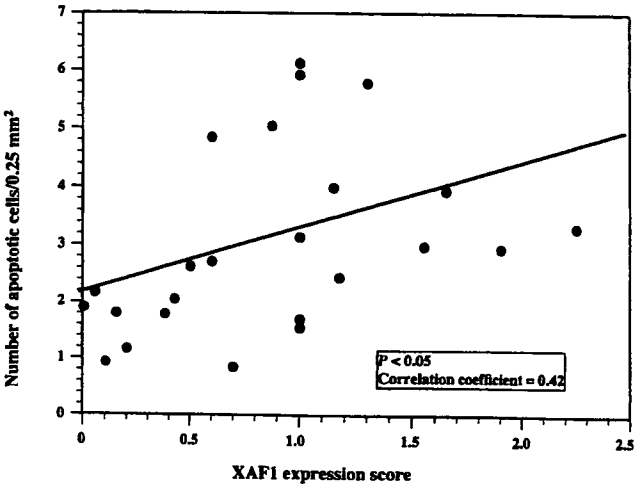

Figure 6. Relationship between the XAF1 expression score and the number of apoptotic tumor cells in hepatocellular carcinoma. Correlation of the coefficient rate is 0.42 ($P<0.05$).

HCC (17). In this study, HCC specimens with an XIAP expression score of 1 (indicating the same staining intensity in cancerous and non-cancerous tissues) or higher accounted for 16/24 (67%), about half of which showed moderate to marked expression, with no significant differentiation-dependent differences [Fig. 4 (left panel)] or relationship between XIAP expression and cancer cell apoptosis.

We examined immunohistochemically the XAF1 protein expression in human HCC tissues and non-HCC tissues. Previous studies revealed that XAF1 mRNA is expressed ubiquitously in all normal adult and fetal tissues including the liver (8,9). In non-HCC tissues, XAF1 was almost homogeneously expressed in non-neoplastic hepatocytes, except in those around the portal areas with active infiltration of inflammatory cells, which showed strong expression. Possible causes of this are: 1) The strong XAF1 expression could be mediated by inflammatory cytokines released from inflammatory cells, Leaman *et al* (19) found that XAF1 mRNA expression is upregulated by inflammatory cytokines, such as interferon (IFN)-γ and tumor necrosis factor-α. 2) Strong XAF1 expression in periportal hepatocytes may be related with the progression of cytotoxic T lymphocyte-induced apoptosis, probably via the Fas/Fas ligand system (16).

In contrast to the normal tissues, XAF1 is present at very low or undetectable levels in a variety of cancer cell lines (8,9), including melanoma (20), colorectal cancer (21), urinary bladder cancer, renal cancer and prostate cancer cell lines (22). In addition, XAF1 mRNA expression in melanoma tissues was significantly reduced compared with benign melanocytic nevi (20), and XAF1 mRNA in primary gastric tumors (14), and bladder transitional cell carcinoma and renal cell carcinoma tissues (22) were substantially lower compared with the non-cancerous tissue. Lee *et al* (22) found that hypermethylation at 14 CpG sites in the 5' proximal region of the XAF1 promoter was highly prevalent in cancers versus adjacent normal or benign tissue and tightly associated with reduced gene expression. Nodules of HCC, particularly well- and moderately differentiated HCCs, were characterized by the heterogeneous (areas of high and low) expression of XAF1, with a tendency toward high expression in HCC cells with fatty change and in the periphery of cancer nodules. On the other hand, XAF1 expression was lower in the poorly differentiated than in the well- and moderately differentiated HCCs. Abnormal reduction of XAF1 mRNA which showed a good correlation with tumor grade, was also reported in gastric and bladder carcinomas (14,22). We found a significant correlation between XAF1 expression and apoptosis; a significant reduction in apoptosis was observed in the poorly differentiated HCCs with a significantly lower expression of XAF1. It has been reported that the relative increase of XIAP to XAF1 expression may provide a survival advantage for tumor cells through the relative increase of XIAP antiapoptotic function (9). XAF1 inactivation in poorly differentiated HCC might contribute to the resistance to apoptosis and malignant progression of HCC. The causes of abnormal expression of XAF1 in HCC require further investigation.

Although this study immunohistochemically demonstrated the expression of XAF1 in the cytoplasm of neoplastic and non-neoplastic hepatocytes, endogenous XAF1 has been reported to be localized in the nucleus (8). However, XAF1 expression has been immunohistochemically detected in both the nucleus and cytoplasm of melanoma and benign nevus cells (20). In addition, its expression has also been noted in the cytoplasm and nucleus of XAF1-transfected 253J cells (22) and IFN-ß-stimulated A375 melanoma cells. Although it is not clear why XAF1 expression was demonstrable only in the cytoplasm in this study, we speculate that the causes of this are related to features specific to hepatocytes and the epitope accessibility of the antibody used. Therefore, further studies need to be performed using cell lines and different antibodies.

Type I IFN, including IFN-α and IFN-ß, has various biologic functions, such as an antiproliferative action (23,24). Recently, XAF1 was identified as an IFN-stimulated gene that contributes to IFN-dependent sensitization of cells to tumor necrosis factor-related apoptosis-inducing ligand-induced apoptosis (19). IFNs induced high levels of XAF1 protein predominantly in cell lines sensitive to the proapoptotic effects of IFN-ß (19). The direct antiproliferative effect of various type I IFN preparations and IFN-α subtypes on HCC cell lines has been reported (25-27) and upregulation of XAF1 mRNA following PEG-IFN-α2b treatment was also observed in the human HCC cell line HAK-1B (unpublished data). In clinical practice, IFN-α in combination with 5-fluorouracil (FU) has been used for the treatment of advanced HCCs, and the recent objective response rate of combination chemotherapy with IFN-α and 5-FU was 52% among HCC patients with portal venous invasion (28). We speculate that XAF1 could be related with the susceptibility to the therapy, and HCCs with the loss or low levels of XAF1 could be more resistant to the combination therapy than HCCs with normal XAF1 expression. Further study is required to examine whether or not XAF1 expression could be a clinically useful marker for the prediction of the outcome of combination chemotherapy with IFN-α and 5-FU.

Acknowledgements

We thank Ms. Sachiyo Maeda and Misato Shiraishi for their assistance in our experiments. This study was supported in

part by the Sarah Cousins Memorial Fund, Boston, MA, and by a Grant-in-Aid from the Ministry of Health, Labor and Welfare of Japan (No. 17200501).

References

1. Nagata S: Apoptosis by death factor. Cell 88: 355-365, 1997.
2. Vaux DL, Haecker G and Strasser A: An evolutionary perspective on apoptosis. Cell 76: 777-779, 1994.
3. Thompson CB: Apoptosis in the pathogenesis and treatment of disease. Science 267: 1456-1462, 1995.
4. Salvesen GS and Duckett CS: IAP proteins: blocking the road to death's door. Nat Rev Mol Cell Biol 3: 401-410, 2002.
5. Deveraux QL, Takahashi R, Salvesen GS and Reed JC: X-linked IAP is a direct inhibitor of cell-death proteases. Nature 388: 300-304, 1997.
6. Holcik M, Gibson H and Korneluk RG: XIAP: apoptotic brake and promising therapeutic target. Apoptosis 6: 253-261, 2001.
7. Tamm I, Kornblau SM, Segall H, *et al*: Expression and prognostic significance of IAP-family genes in human cancers and myeloid leukemias. Clin Cancer Res 6: 1796-1803, 2000.
8. Fong WG, Liston P, Rajcan-Separovic E, St Jean M, Craig C and Korneluk RG: Expression and genetic analysis of XIAP-associated factor 1 (XAF1) in cancer cell lines. Genomics 70: 113-122, 2000.
9. Liston P, Fong WG, Kelly NL, *et al*: Identification of XAF1 as an antagonist of XIAP anti-Caspase activity. Nat Cell Biol 3: 128-133, 2001.
10. Verhangen AM, Ekert PG, Pakusch M, *et al*: Identification of DIABLO, a mammalian protein that promotes apoptosis by binding to and antagonizing IAP proteins. Cell 102: 43-53, 2000.
11. Du C, Fang M, Li Y, Li L and Wang X: Smac, a mitochondrial protein that promotes cytochrome c-dependent caspase activation by eliminating IAP inhibition. Cell 102: 33-42, 2000.
12. Liu Z, Sun C, Olejniczak ET, *et al*: Structural basis for binding of Smac/DIABLO to the XIAP BIR3 domain. Nature 408: 1004-1008, 2000.
13. Wu G, Chai J, Suber TL, Wu JW, Du C, Wang X and Shi Y: Structural basis of IAP recognition by Smac/DIABLO. Nature 408: 1008-1012, 2000.
14. Byun DS, Cho K, Ryu BK, Lee MG, Kang MJ, Kim HR and Chi SG: Hypermethylation of XIAP-associated factor 1, a putative tumor suppressor gene from the 17p13.2 locus, in human gastric adenocarcinomas. Cancer Res 63: 7068-7075, 2003.
15. Yano H, Fukuda K, Haramaki M, Momosaki S, Ogasawara S, Higaki K and Kojiro M: Expression of Fas and anti-Fas-mediated apoptosis in human hepatocellular carcinoma cell lines. J Hepatol 25: 454-464, 1996.
16. Higaki K, Yano H and Kojiro M: Fas antigen expression and its relationship with apoptosis in human hepatocellular carcinoma and non-cancerous tissues. Am J Pathol 149: 429-437, 1996.
17. Shiraki K, Sugimoto K, Yamanaka Y, *et al*: Overexpression of X-linked inhibitor of apoptosis in human hepatocellular carcinoma. Int J Mol Med 12: 705-708, 2003.
18. Vischioni B, van der Valk P, Span SW, Kruyt FA, Rodriguez JA and Giaccone G: Expression and localization of inhibitor of apoptosis proteins in normal human tissues. Hum Pathol 37: 78-86, 2006.
19. Leaman DW, Chawla-Sarkar M, Vyas K, Reheman M, Tamai K, Toji S and Borden EC: Identification of X-linked inhibitor of apoptosis-associated factor-1 as an interferon-stimulated gene that augments TRAIL Apo2L-induced apoptosis. J Biol Chem 277: 28504-28511, 2002.
20. Ng KC, Campos EI, Martinka M and Li G: XAF1 expression is significantly reduced in human melanoma. J Invest Dermatol 123: 1127-1134, 2004.
21. Ma TL, Ni PH, Zhong J, Tan JH, Qiao MM and Jiang SH: Low expression of XIAP-associated factor 1 in human colorectal cancers. Chin J Dig Dis 6: 10-14, 2005.
22. Lee MG, Huh JS, Chung SK, *et al*: Promoter CpG hypermethylation and downregulation of XAF1 expression in human urogenital malignancies: implication for attenuated p53 response to apoptotic stresses. Oncogene 25: 5807-5822, 2006.
23. Pestka S, Langer JA, Zoon KC and Samuel CE: Interferons and their actions. Ann Rev Biochem 56: 727-777, 1987.
24. Gutterman JU: Cytokine therapeutics: lessons from interferon α. Proc Natl Acad Sci USA 91: 1198-1205, 1994.
25. Yano H, Yanai Y, Momosaki S, *et al*: Growth inhibitory effects of interferon-α subtypes vary according to human liver cancer cell lines. J Gastroenterol Hepatol 21: 1720-1725, 2006.
26. Yano H, Ogasawara S, Momosaki S, *et al*: Growth inhibitory effects of pegylated IFN α-2b on human liver cancer cells *in vitro* and *in vivo*. Liver Int 26: 964-975, 2006.
27. Yano H, Iemura A, Haramaki M, Ogasawara S, Takayama A, Akiba J and Kojiro M: Interferon alfa receptor expression and growth inhibition by interferon alfa in human liver cancer cell lines. Hepatology 29: 1708-1717, 1999.
28. Obi S, Yoshida H, Toune R, *et al*: Combination therapy of intraarterial 5-fluorouracil and systemic interferon-alpha for advanced hepatocellular carcinoma with portal venous invasion. Cancer 106: 1990-1997, 2006.

JOURNAL OF INTERFERON & CYTOKINE RESEARCH 27:507–516 (2007)

DOI: 10.1089/jir.2007.0183

Growth Inhibitory Effects of IFN-β on Human Liver Cancer Cells *In Vitro* and *In Vivo*

SACHIKO OGASAWARA, HIROHISA YANO, SEIYA MOMOSAKI, JUN AKIBA, NAOYO NISHIDA, SAKIKO KOJIRO, FUKUKO MORIYA, HIRONORI ISHIZAKI, KEITARO KURATOMI, and MASAMICHI KOJIRO

ABSTRACT

We investigated the effects of interferon-β (IFN-β) on the growth of human liver cancer cells. The effects of IFN-β with or without 5-fluorouracil (5-FU) on the proliferation of 13 liver cancer cell lines were investigated *in vitro*. Chronologic change in IFN-α receptor 2 (IFNAR-2) expression was monitored in hepatocellular carcinoma (HCC) cells (HAK-1B) cultured with IFN-β. After HAK-1B cells were transplanted into nude mice, various doses of IFN-β were administered, and the tumor volume, weight, histology, tumor blood vessel, and angiogenesis factor expression were examined. IFN-β inhibited the growth of 11 cell lines with apoptosis in a dose-dependent and time-dependent manner. With IFN-β, IFNAR-2 expression in HAK-1B cells was significantly downregulated from 6 to 12 h. IFN-β induced a dose-dependent decrease in tumor volume and weight and a significant increase of apoptosis in the tumor. Both basic fibroblast growth factor (bFGF) and blood vessel number in the tumor decreased only in mice receiving the lowest dose (1000 IU) of IFN-β. IFN-β with 10 μM of 5-FU frequently induced synergistic antiproliferative effects. IFN-β with or without 5-FU induces strong antitumor effects in HCC cells, and we conclude that IFN-β is useful for the prevention and treatment of HCC.

INTRODUCTION

Interferons (IFNs) are a family of cytokines that possess various biologic activities, such as antiviral, antiproliferative, antiangiogenetic, immunomodulatory, and antitelomerase activities.[1–3] IFNs are classified into two major groups, type I IFN that includes IFN-α, IFN-β, and IFN-ω, and type II IFN, IFN-γ.[4] Both type I and type II IFNs bind with distinct cellular receptors and activate distinct and overlapping pathways.[5]

Hepatocellular carcinoma (HCC) is one of the most frequently found primary cancers, and many HCC patients have chronic hepatitis or cirrhosis caused by chronic infection with hepatitis B virus (HBV) or hepatitis C virus (HCV) as their background disease.[6–8] IFN-α and IFN-β have been used in the treatment of virus-related chronic hepatitis to eradicate these viruses. Recently, IFN-α and IFN-β have been shown to possess highly suppressive effects on hepatocellular carcinogenesis and on the recurrence of HCC after curative treatment in patients with virus-related chronic hepatitis.[9–13] The precise mechanisms of these suppressive actions have not yet been clarified, but direct antiproliferative effects of IFN-α and IFN-β may be involved. As IFN-α and IFN-β have various antitumor properties, they have been used in the treatment of such malignant diseases as melanoma, renal cell carcinoma (RCC), and chronic myelogeneous leukemia (CML).[14–16] Recent studies reported that administration of IFN-α in combination with chemotherapeutic agents, such as 5-fluorouracil (5-FU), was also effective against advanced HCC cases, including those showing tumor invasion into the major branches of the portal vein.[17–19]

Many researchers have investigated the antiproliferative effects and action mechanisms of IFN-α *in vitro* and *in vivo* by using liver cancer cell lines.[20–27] We have reported that (1) each IFN-α preparation or subtype presents very different antiproliferative activities in different human HCC cell lines, (2) a common mechanism of *in vitro* growth suppression by IFN-α is cell cycle arrest with or without caspase-dependent apoptosis induction, and (3) the mechanism of *in vivo* growth inhibi-

Department of Pathology, Kurume University School of Medicine, and Research Center of Innovative Cancer Therapy of the 21st Century COE Program for Medical Science, Kurume University, Kurume 830-0011, Japan.

tion by IFN-α is the induction of apoptosis with or without inhibition of angiogenesis.[20–24] However, IFN-β, another important IFN that is also used in treatment of chronic virus-related hepatitis, has not been investigated in as much detail as IFN-α, and there have been only a few basic *in vitro* studies published in the literature.[28–30] Therefore, its antitumor properties on HCC cells *in vitro* and *in vivo* remain to be clarified. In the current study, we investigated (1) the antiproliferative effects of IFN-β on liver cancer cell lines *in vitro* and *in vivo*, (2) chronologic changes in the expression of type I IFN receptor 2 (IFNAR-2) subunit and its relationship with antitumor effects on HCC cells treated with IFN-β, and (3) the antiproliferative effects of IFN-β alone or in combination with 5-FU on liver cancer cell lines *in vitro*.

MATERIALS AND METHODS

Cell lines and cell culture

This study used 11 HCC cell lines (KIM-1, KYN-1, KYN-2, KYN-3, HAK-1A, HAK-1B, HAK-2, HAK-3, HAK-4, HAK-5, and HAK-6) and 2 human combined hepatocellular and cholangiocarcinoma (CHC) cell lines (KMCH-1 and KMCH-2). These HCC and CHC cell lines were originally established in our laboratory, and each cell line retains the morphologic and functional features of the original tumor as described elsewhere.[31–39] The cells were grown in Dulbecco's modified Eagle's medium (DMEM) (Nissui Seiyaku, Tokyo, Japan) supplemented with 2.5% heat-inactivated (56°C, 30 min) fetal bovine serum (FBS) (Bioserum, Victoria, Australia), 100 U/mL penicillin, 100 μg/mL streptomycin (GIBCO-BRL/Life Technologies, Inc., Gaithersburg, MD), and 12 mmol/L sodium bicarbonate in a humidified atmosphere of 5% CO_2 in air at 37°C.

IFN and reagents

IFN-β (FERON) was kindly provided by Toray Industries (Tokyo, Japan), and the specific activity of IFN-β was 2×10^8 IU/mg protein. 5-FU was purchased from Kyowa Hakko Co. (Tokyo, Japan), fluorescein isothiocyanate-conjugated goat anti-mouse immunoglobulin (FITC-GAM) was from BD Biosciences (San Jose, CA), control normal mouse IgG1 was from DAKO (Glostrup, Denmark); rat antibody against mouse endothelial cells (anti-CD34, clone MEC14.7) was from Serotec Ltd. (Oxford, U.K.), mouse monoclonal antibody (mAb) against human α-smooth muscle actin (SMA) that cross-reacts with mouse α-SMA (clone 1A4) was from Immunon (Pittsburgh, PA), and mouse mAb against human IFNAR-2 was from Chemicon International (Temecula, CA).

Effects of IFN-β on proliferation of HCC and CHC cell lines in vitro

The effects of IFN-β on the growth of the cultured cells were examined with colorimetry using 3-(4,5-dimethylthiazol-2yl)-2,5-diphenyl tetrazolium bromide (MTT) assay kits (Chemicon) as described elsewhere.[20,24] Briefly, the cells ($1.5–6 \times 10^3$ cells/well) were seeded onto 96-well plates (Nunc, Roskilde, Denmark) and cultured for 24 h, and the culture medium was changed to new medium with or without IFN-β (16, 64, 256, 1024, or 4096 IU/mL). After culture for 24, 48, 72, or 96 h, the number of viable cells was examined.

Morphologic observation

For morphologic observation under a light microscope, cultured cells were seeded on Lab-Tek tissue culture chamber slides (Nunc), cultured with or without IFN-β (256, 1024 or 4096 IU/mL) for 48 or 72 h, fixed for 10 min in Carnoy's solution, and stained with hematoxylin-eosin (HE).

Quantitative analysis of IFN-β-induced apoptosis in vitro

Cells cultured with or without 1000 IU/mL (IFN-β) for 72 h were stained with Annexin V-enhanced green fluorescent protein (EGFP) apoptosis detection kits (Medical & Biological Laboratories, Nagoya, Japan) according to the manufacturer's protocol. After staining, the cells were analyzed using a FACScan (Becton Dickinson Immunocytometry Systems, San Jose, CA), and the Annexin V-EGFP-positive apoptotic cell rate was determined.

Effects of IFN-β on proliferation and expression of IFNAR-2 subunit

To investigate the expression of the IFNAR-2 subunit after contact with IFN-β, as well as its relationship with antiproliferative effects, HAK-1B cells were cultured with medium alone (control group) or medium containing 1000 IU/mL IFN-β for 3, 6, 12, 24, 48, or 72 h. The cells were reacted with anti-IFNAR-2 antibody (final concentration 2.5 μg/mL) or control antibody. The cell surface expression of the IFNAR-2 subunit was analyzed using flow cytometry with the technique described elsewhere,[20,21] with slight modification.

Effects of IFN-β on HCC cell proliferation in nude mice

This experiment was conducted according to the *Guide for the Care and Use of Laboratory Animals* published and revised by the National Institutes of Health in 1985. HAK-1B cells (1.0×10^7 cells/mouse) were transplanted subcutaneously (s.c.) into 4-week-old female BALB/c nu/nu athymic nude mice. Eight days later, when the largest diameter of the tumor reached approximately 5–10 mm, the mice were divided into four groups ($n = 10$ each) to balance the mean tumor diameter of each group. Each mouse received an intraperitoneal (i.p.) injection of 0.1 mL phosphate-buffered saline (PBS) containing 1,000, 10,000, or 100,000 IU IFN-β for 14 consecutive days. The clinical dose of IFN-β in chronic hepatitis C treatment is about 1.2×10^5 IU/kg and is 2.4 times the lowest dose (5.0×10^4 IU/kg) in the experiment. During this 2-week period, tumor size was measured in two directions using calipers once every 2 days until day 15, and tumor volume (mm^3) was estimated using the equation: length $\times$ $(\text{width})^2 \times 0.5$. On day 15, the mice were killed, and the tumors were resected, weighed, and used for morphologic studies and ELISA analysis. Half of the resected tumor was fixed in formalin and prepared in paraffin sections. The TUNEL method using ApopTag kit (S7100, Chemicon) was used to detect apoptotic cells. The number of apoptotic cells was counted in ten 0.25-mm^2 areas where apoptotic cells

were present at relatively uniform density, and the average number per area was obtained. To compare the *in vivo* antitumor effect according to the administration route, IFN-β was administered i.v., and tumor volume and weight were examined as described.

Quantification of microvessel density

Double-immunostaining was performed with antimouse endothelial cell antibody, antihuman α-SMA antibody, Histofine simple stain mouse MAX-PO (Rat) kits (Nichirei, Tokyo, Japan), and HistoMouse-plus kits to detect arterylike blood vessels as described in our previous report.[21] The number of blood vessels in the tumor and in the borderline area between the tumor nodule and surrounding tissues was counted on each specimen. The size of the counted area was measured by tracing the outline displayed on a computer monitor using Mac SCOPE (Mitani Corp., Chiba, Japan). From the obtained number of vessels per unit area (mm^2), the group mean was obtained for group comparison.

Enzyme-linked immunosorbent assay (ELISA)

Portions of the resected tumors were cut into pieces, and an appropriate amount was homogenized in 500 μL ice-cold Ca^{2+}- and Mg^{2+}-free PBS containing 100 μg/mL phenymethylsulfonyl fluoride (PMSF) using a pellet pestle. The mixture was centrifuged for 10 min (12,000*g*, 4°C), and the supernatant was stored at −20°C until use. The amount of tissue protein was determined using BCA protein assay reagent (Pierce Biotechnology, Rockford, IL). The concentration in the samples was determined by comparing their absorbance with a standard curve. The amount of basic fibroblast growth factor (bFGF), interleukin-8 (IL-8), and vascular endothelial growth factor (VEGF) in the supernatant was measured using ELISA kits. The kits for VEGF and IL-8 were supplied by Amersham Biosciences (Buckinghamshire, U.K.), and those for bFGF by R&D Systems (Minneapolis, MN).

Effects of IFN-β and 5-FU on proliferation of HCC and CHC cell lines in vitro

The cells (1.5–6 × 10^3 cells/well) were seeded on 96-well plates and cultured for 24 h, and then the culture medium was changed to fresh medium containing IFN-β (0, 8, 40, 200, or 100 IU/mL), 5-FU (0, 1, 10, or 100 μM), or both IFN-β (0, 8, 40, 200, or 100 IU/mL) and 5-FU (0, 1, 10, or 100 μM). After 72 h of culture, the number of viable cells was examined with colorimetry using MTT assay kits as described. The synergy of cooperative cytotoxicity was determined by the median-effect principle as described by Chou and Talalay.[40] Data from each sample were analyzed using CalcuSyn ver. 2 (Biosoft, Cambridge, U.K.).

Statistical analysis

Estimated tumor volume and colorimetric cell growth were compared using two-factor factorial ANOVA and Student's *t*-test, respectively. The other data comparisons were performed using the Mann-Whitney U-test.

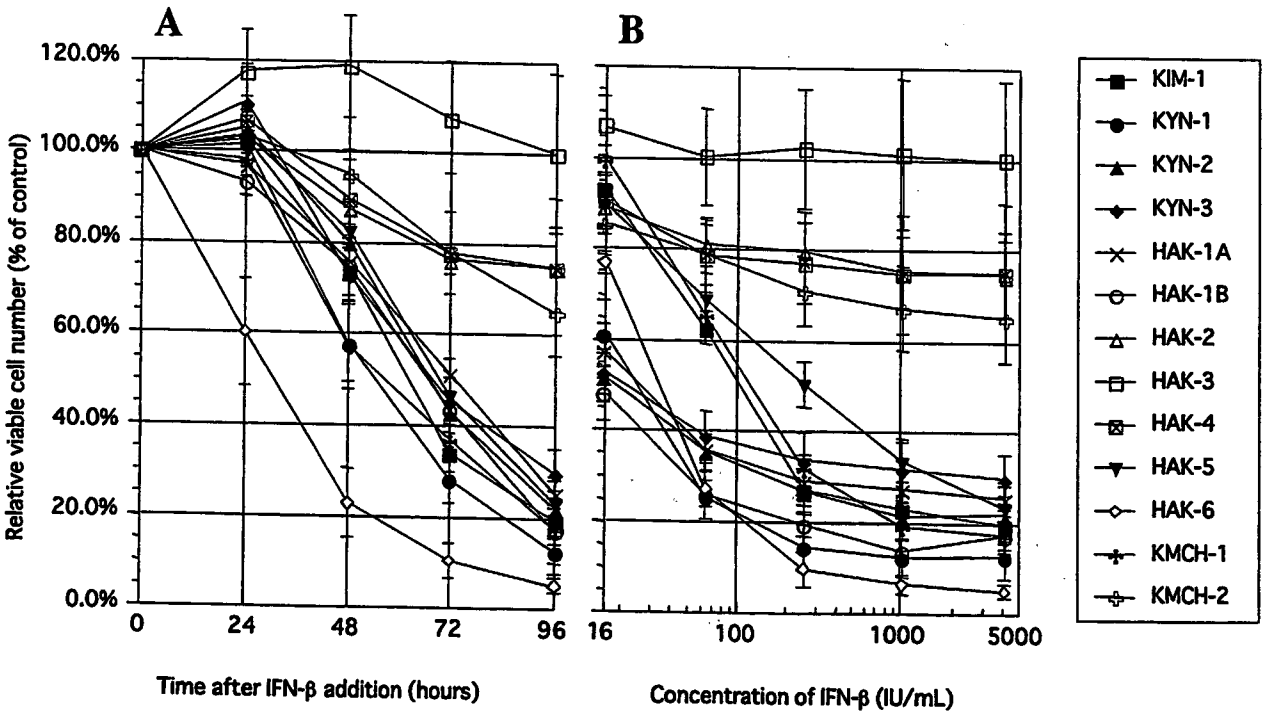

FIG. 1. Antiproliferative effect of IFN-β. (**A**) Chronologic changes in the relative viable cell number (% of the control) after adding 4096 IU/mL IFN-β. Growth was suppressed with time in 12 cell lines. (**B**) 96 h after adding 16, 64, 256, 1024, or 4,096 IU/mL IFN-β. Cell proliferation was suppressed in a dose-dependent manner in 11 cell lines. Suppression was statistically significant ($p <$ 0.001–0.05) in the range of 16–4096 IU/mL IFN-β in 8 cell lines. Eight samples were used in each experiment ($n = 8$). The experiment was repeated at least three times for each cell line. The figures represent average ± SE of the experiments.

RESULTS

Effects of IFN-β on liver cancer cell proliferation in vitro

In 12 of the 13 cell lines, a time-dependent antiproliferative effect was observed at various degrees in the 96-h cultures with 4096 IU/mL of IFN-β, and 20% or more suppression occurred at 72 h or later in comparison to the control (Fig. 1A). Among the 12 cell lines, HAK-6 presented a different pattern, and the cell number started to decrease from the early culture period after the addition of IFN-β, decreasing to 60% of the control at 24 h. On the other hand, HAK-3 did not have suppressive effects at 96 h.

The relative viable cell number at 96 h after adding IFN-β (16, 64, 256, 1024, or 4096 IU/mL) decreased in 11 of the 13 cell lines in a dose-dependent manner (Fig. 1B). The cell lines that did not have effects were HAK-3 and HAK-4. Among the 11 cell lines, cell number was suppressed in the 6 cell lines (KYN-1, KYN-2, KYN-3, HAK-1A, HAK-1B, and HAK-6) to <40% of the control even at a very low dose (64 IU/mL), and the suppression was statistically significant in 8 cell lines in the dose range between 16 and 4096 IU/mL ($p < 0.001$–0.05). The 50% inhibitory concentration (IC_{50}) was 14.8 IU/mL for KYN-2, 15.4 for HAK-1B, 25.2 for KYN-3, 31.2 for KYN-1, 32.5 for HAK-1A, 42.0 for HAK-6, 132.0 for KIM-1, 152.7 for KMCH-1, and 260.1 for HAK-5. There was no significant relationship between the histologic differentiation level of the original tumor of each cell line and sensitivity to the antiproliferative effect of IFN-β.

Between 48 and 72 h after adding 4096 IU/mL IFN-β, 10 cell lines (all but HAK-3, HAK-4, and KMCH-2) presented such characteristic features of apoptosis as cytoplasmic shrinkage, chromatin condensation, and nuclear fragmentation to various degrees (Color Plate 1).

Quantitative analysis of Annexin V-EGFP-positive apoptotic cells revealed that apoptosis occurred at a significantly higher rate in the cultures with 1000 IU/mL IFN-β than those without IFN-β in 10 cell lines (Table 1).

Effects of IFN-β in vitro *on proliferation and expression of IFNAR-2 in HAK-1B cells*

With IFN-β, the expression of IFNAR-2 in HAK-1B cells was significantly downregulated in the period between 6 and 12 h in comparison to the control, then significantly upregulated at 48 h and returned to the control level at 72 h (Fig. 2). The number of viable cells between 3 and 12 h was almost the same in both the control and the culture with IFN-β, started to decrease after 24 h in the IFN-β group, and decreased to 16.1% of the control at 72 h.

Effects of IFN-β on HCC cell proliferation in nude mice

Figure 3A summarizes the chronologic changes in estimated tumor volume after s.c. injection of cultured HAK-1B cells to nude mice. A significant difference in the time course change was obtained between the control mice and the mice that received 1,000 ($p < 0.05$), 10,000 ($p < 0.0001$), or 100,000 IU ($p < 0.0001$) IFN-β by two-factor factorial ANOVA. Dose-dependent suppression of tumor volume was also observed, and HAK-1B tumor on day 15 was smaller in proportion to the dose (Fig. 3A). A significant difference was obtained in the tumor weight between the control and the 10,000 IU/mouse group ($p < 0.05$) and 100,000 IU/mouse group ($p < 0.001$). The tumor weight of the 100,000 IU/mouse group was 40.0% of the control. Similar antitumor effects were obtained when IFN-β was administered i.v. (data not shown).

TUNEL staining showed that the numbers of apoptotic cells in the 10,000 IU and 100,000 IU IFN-β groups were significantly higher than that of the control, and the number increased in a dose-dependent manner (Color Plate 2 and Table 2) ($p <$ 0.0001 between 10,000 or 100,000 group vs. Control).

Expression of angiogenesis factors and density of arterylike blood vessels

VEGF expression in the HAK-1B tumor was higher in mice that received IFN-β and was significantly higher in the 10,000 IU IFN-β group ($p < 0.05$) than the control (Table 2). IL-8 expression in the tumor was not significantly different among the groups. bFGF expressions in both tumor and serum were significantly lower in the 1,000 IFN-β group ($p < 0.05$) than the control, and IL-8 expressions in serum were significantly lower in all IFN-β groups ($p < 0.0001$).

There were no significant differences in the number of blood vessels per unit area of the HAK-1B tumor among all groups, but the blood vessel counts inside the tumor tended to be lower in the 1,000 IU IFN-β group (Table 2).

Antiproliferative effects of IFN treatment in combination with 5-FU

Seventy-two hours after the addition of 5-FU alone, the relative viable cell number was suppressed in all 13 cell lines in a dose-dependent manner. The combination treatment of IFN-β and 5-FU showed synergistic antiproliferative effects in all

TABLE 1. QUANTITATIVE ANALYSIS OF APOPTOSIS INDUCED BY IFN-β IN 13 LIVER CANCER CELL LINES[a]

	Annexin V-EGFP-positive apoptotic cells (%)	
Cell line	*Control*	*IFN-β*
KIM-1	6.9 ± 3.6	36.2 ± 2.3**
KYN-1	10.2 ± 0.7	24.2 ± 1.3**
KYN-2	8.1 ± 1.3	28.2 ± 4.3**
KYN-3	6.3 ± 1.5	17.1 ± 3.7**
HAK-1A	8.7 ± 0.8	19.1 ± 0.7**
HAK-1B	8.7 ± 3.7	30.4 ± 2.9**
HAK-2	11.9 ± 2.4	21.6 ± 1.9*
HAK-3	4.8 ± 0.9	8.9 ± 1.5
HAK-4	5.9 ± 2.3	6.9 ± 0.8
HAK-5	3.7 ± 0.5	20.9 ± 1.9**
HAK-6	11.5 ± 2.9	33.6 ± 2.6**
KMCH-1	6.5 ± 1.0	18.3 ± 1.2**
KMCH-2	7.8 ± 2.6	7.4 ± 3.0

[a]Cells were cultured with medium alone (Control) or medium with 1000 IU/mL IFN-β. Apoptosis was measured by Annexin V-EGFP staining. The rates of Annexin V-EGFP-positive apoptotic cells are shown as the average ± SD. Five samples were used in each experiment.

*$p < 0.001$ vs. corresponding control value.

**$p < 0.0001$ vs. corresponding control value.

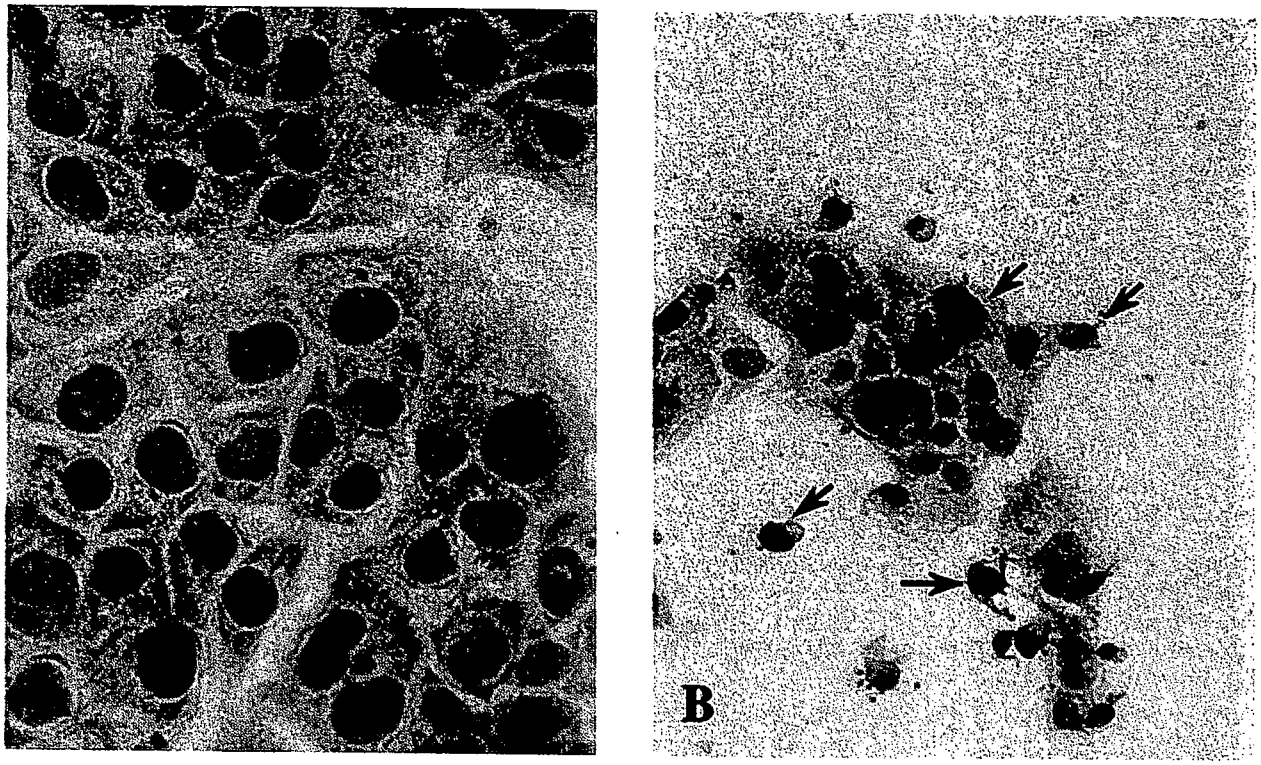

COLOR PLATE 1. Photomicrograph of HAK-1B cells cultured for 48 h on a Lab-Tek chamber slide (**A**) without IFN-β in culture medium and (**B**) with 4096 IU/mL IFN-β in culture medium. Apoptotic cells (arrows) characterized by cytoplasmic shrinkage, chromatic condensation, and nuclear fragmentation were noted. HE staining ×200.

cell lines, but the frequency of the effect and the suitable combination of each drug concentration depended on the cell lines. Synergistic effects were observed most frequently at 10 μM 5-FU in all cell lines excluding KMCH-2 (Fig. 4); however, in three cell lines (HAK-1A, HAK-1B, and HAK-2), synergistic effects were observed with high frequency at all 5-FU concentrations tested.

DISCUSSION

This study showed that (1) a time-dependent antiproliferative effect was induced in 12 cell lines that had contact with 4096 IU/mL IFN-β for 24–96 h and (2) a dose-dependent antiproliferative effect was induced in 11 cell lines *in vitro* in the range of 16–4096 IU/mL. We previously reported the antipro-

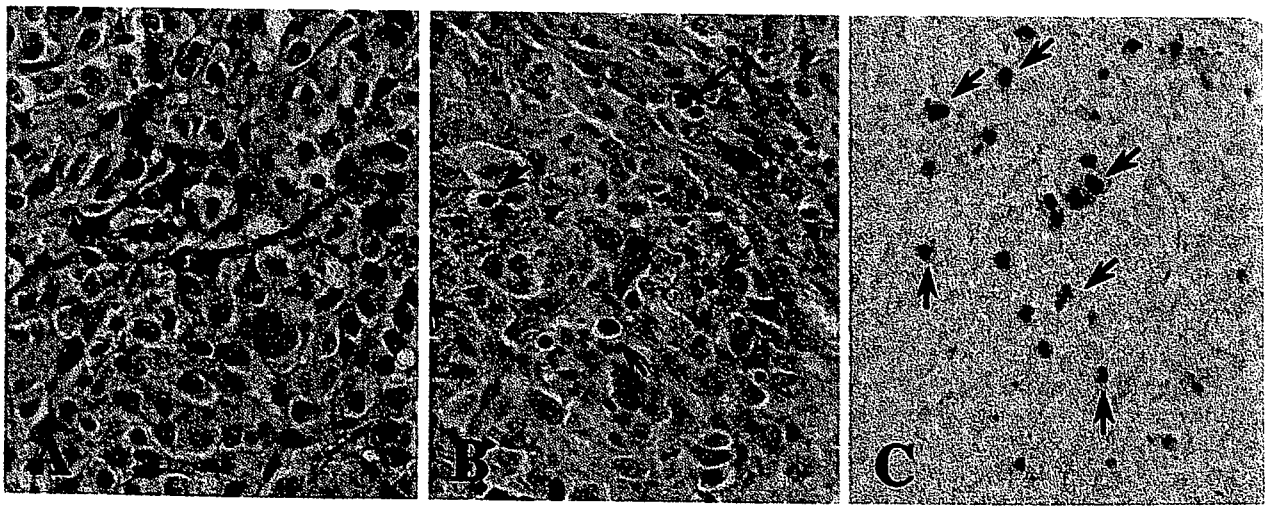

COLOR PLATE 2. Photomicrograph of subcutaneous human HCC tumor in nude mice that developed after the injection of HAK-1B cells. (**A**) Control mouse that received culture medium alone. Tumor shows a thick trabecular arrangement of tumor cells and a sinusoidlike structure in the stroma. (**B**) Mouse that received an i.p. injection of 100,000 IU IFN-β. There are many apoptotic tumor cells (arrows). HE staining. ×200. (**C**) TUNEL technique was used to identify apoptotic cells (arrows). Counterstained with Mayer's hematoxylin. ×200.